

NH Acids

Fluoro- and Perfluoralkylsulfonylpentafluoroanilides: Synthesis and Characterization of NH Acids for Weakly Coordinating Anions and Their Gas-Phase and Solution Acidities

Julius F. Kögel,^[a] Thomas Linder,^[a] Fabian G. Schröder,^[a] Jörg Sundermeyer,^{*[a]} Sascha K. Goll,^[b] Daniel Himmel,^[b] Ingo Krossing,^{*[b]} Karl Kütt,^[c] Jaan Saame,^[c] and Ivo Leito^{*[c]}

Abstract: Fluoro- and perfluoralkylsulfonyl pentafluoroanilides [$\text{HN}(\text{C}_6\text{F}_5)(\text{SO}_2\text{X})$; $\text{X}=\text{F}, \text{CF}_3, \text{C}_4\text{F}_9, \text{C}_8\text{F}_{17}$] are a class of imides with two different strongly electron-withdrawing substituents attached to a nitrogen atom. They are NH acids, the unsymmetrical hybrids of the well-known symmetrical bisulfonylimides and bispentafluorophenylamine. The syntheses, the structures of these perfluoroanilides, their solvates, and some selected lithium salts give rise to a structural variety beyond the symmetrical parent compounds. The acidities of representative subsets of these novel NH acids have been investigated experimentally and quantum-chemically and their gas-phase acidities (GAs) are reported, as well as the pK_a values of these compounds in acetonitrile (MeCN) and DMSO solution. In quantum chemical investigations with the vertical and relaxed COSMO cluster-continuum models (vCCC/rCCC), the unusual situation is encountered

that the DMSO-solvated acid $\text{Me}_2\text{SO}-\text{H}-\text{N}(\text{SO}_2\text{CF}_3)_2$, optimized in the gas phase (vCCC model), dissociates to $\text{Me}_2\text{SO}-\text{H}^+-\text{N}(\text{SO}_2\text{CF}_3)_2^-$ during structural relaxation and full optimization with the solvation model turned on (rCCC model). This proton transfer underlines the extremely high acidity of $\text{HN}(\text{SO}_2\text{CF}_3)_2$. The importance of this effect is studied computationally in DMSO and MeCN solution. Usually this effect is less pronounced in MeCN and is of higher importance in the more basic solvent DMSO. Nevertheless, the neglect of the structural relaxation upon solvation causes typical changes in the computational pK_a values of 1 to 4 orders of magnitude (4–20 kJ mol⁻¹). The results provide evidence that the published experimental DMSO pK_a value of $\text{HN}(\text{SO}_2\text{CF}_3)_2$ should rather be interpreted as the pK_a of a $\text{Me}_2\text{SO}-\text{H}^+-\text{N}(\text{SO}_2\text{CF}_3)_2^-$ contact ion pair.

1. Introduction

Bis(trifluoromethanesulfonyl)imide ($\text{HN}(\text{SO}_2\text{CF}_3)_2$ or HNTf_2) was first described by DesMarteaum in 1984.^[1] Since then, it has attracted most scientific interest among the NH-acidic compounds. Its extraordinary Brønsted acidity is caused by the two strongly electron-withdrawing triflyl (CF_3SO_2^- , Tf^-) moieties

and has been examined in various theoretical and experimental works.^[2] It has been applied in numerous Brønsted acid-catalyzed reactions like Diels–Alder reactions,^[3] hetero-Michael additions,^[4] cyclization of siloxyalkynes with arenes and alkenes,^[5] or imine amidation reactions.^[6] Due to its weakly coordinating nature, the corresponding anion $[\text{NTf}_2]^-$ is widely used in imidazolium-,^[7] pyrrolidinium-,^[8] guanidinium-^[9] or phosphonium-based^[10] ionic liquids with low melting points, which can serve as reaction media^[11] or components of electrochemical devices.^[12] Furthermore, $[\text{NTf}_2]^-$ can act as a ligand, generating extremely electron-poor and therefore highly Lewis-acidic metal centers that have been successfully tested in Lewis acid-catalyzed reactions.^[13] Other applications of its metal complexes include the field of materials for gas absorption^[14] or luminescent lanthanide complexes.^[15] The related fluorosulfonylimide $\text{HN}(\text{SO}_2\text{F})_2$ has also been a prominent subject of theoretical and electrochemical investigations.^[16] Although less acidic by more than ten orders of magnitude than both sulfonylimides, decafluorodiphenylamine $\text{HN}(\text{C}_6\text{F}_5)_2$ is another well-known representative of the nitrogen acid family.^[17] Research to date has focused on its use as a weakly basic and sterically demanding amido ligand for transition metals,^[18] lanthanides^[19] and main group metals.^[20] The sterically demanding aryl substituents

[a] J. F. Kögel, T. Linder, F. G. Schröder, J. Sundermeyer
Fachbereich Chemie der Philipps-Universität
Wissenschaftliches Zentrum für Materialwissenschaften (WZMW) Marburg
Hans-Meerwein-Str., 35043 Marburg (Germany)
E-mail: jsu@staff.uni-marburg.de

[b] S. K. Goll, D. Himmel, I. Krossing
Institut für Anorganische und Analytische Chemie
Freiburger Materialforschungszentrum (FMF) and Freiburg Institute for Advanced Studies (FRIAS), Section Soft Matter Science
Universität Freiburg, Albertstr. 21, 79104 Freiburg (Germany)
E-mail: ingo.krossing@ac.uni-freiburg.de

[c] K. Kütt, J. Saame, I. Leito
University of Tartu, Institute of Chemistry
Ravila 14a, 50411 Tartu (Estonia)
E-mail: ivo.leito@ut.ee

 Supporting information for this article is available on the WWW under <http://dx.doi.org/10.1002/chem.201405391>.

provide a shielding of the Lewis acidic metal centers and chelating coordination of the *ortho*-fluorine atoms can lead to an increase in the coordination number through secondary metal–fluorine contacts. Additionally, ionic liquids with the rather naked amide anion $[N(C_6F_5)_2]^-$ have been prepared and structurally characterized.^[21]

This report concerns hybrids of both classes of NH acids, namely $HN(C_6F_5)(SO_2Rf)$ ($Rf=F, CF_3, C_4F_9$, or C_8F_{17}). For easier notation, the following abbreviations are used: $C_6F_5=Pf$, $SO_2F=Sf$, $SO_2CF_3=Tf$, $SO_2C_4F_9=Nf$ and $SO_2C_8F_{17}=Hf$ (Figure 1).

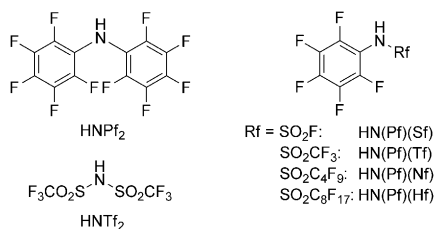


Figure 1. Symmetric and asymmetric NH acids investigated in this work.

The syntheses of these molecules are reported, their molecular structures as pure acid, as solvate, or as lithium salt are presented, and pK_a values in MeCN are experimentally determined. Additionally, the Gibbs solvation energies and pK_a values in MeCN and DMSO are also calculated with the high-level vertical and relaxed COSMO cluster-continuum (vCCC and rCCC) models. Unusually, the DMSO-solvated $HNTf_2$ acid dissociated upon optimization in the solvent, and neglect of this effect led to a pK_a value erroneous by 10 orders of magnitude. Therefore, the importance of accounting for possible dissociation of the acid upon solvation during computations has also been studied for an exemplarily chosen set of systems in DMSO and MeCN. It should be noted that these investigations would have been impossible without the experimental input.

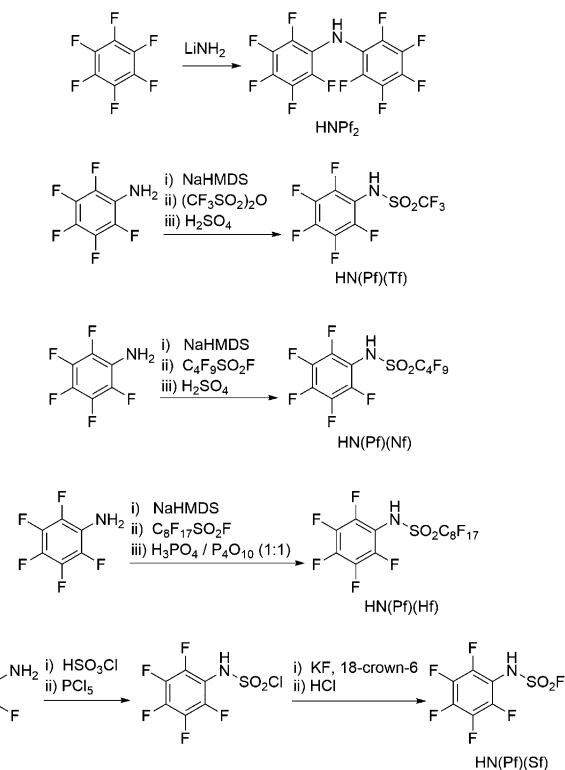
2. Results and Discussion

2.1. Synthesis and characterization of fluoro- and perfluoroalkylsulfonyl pentafluoroanilides

2.1.1. Synthesis

Herein, we provide a full account of an optimized procedure to synthesize $HN(Pf)(Tf)$, which, in preliminary communications, has been used as an anion-generating acid for various highly lipophilic ionic liquids^[21] and thermally stable, as well as electrochemically suitable, lithium electrolyte systems.^[22] The reaction of C_6F_5NHNa generated *in situ* from pentafluoroaniline and $NaN(SiMe_3)_2$ with $(CF_3SO_2)_2O$ gives the sodium salt $NaN(Pf)(Tf)$ and one equivalent of sodium triflate. If only one equivalent of the base $NaN(SiMe_3)_2$, instead of two, is applied in this synthesis, the acidic product $HN(Pf)(Tf)$ quenches the nucleophile C_6F_5NHNa and, as a result, the yield does not exceed the theoretical maximum of 50%. After protonation of this salt mixture with sulfuric acid followed by sublimation, the pure nitrogen acid is obtained as colorless solid. It is slightly

hygroscopic and fuming in the air. The higher homologues with nonafluorobutyl and heptadecafluoroctyl chains, $HN(Pf)(Nf)$ and $HN(Pf)(Hf)$, are generated in analogous procedures using the sulfonylfluorides $C_4F_9SO_2F$ and $C_8F_{17}SO_2F$ as S-electrophiles. In case of $HN(Pf)(Hf)$, protonation of the corresponding sodium salt is preferably carried out with *meta*-phosphoric acid prepared from mixing H_3PO_4 (85%) and P_4O_{10} . The less volatile the NH acid, the more difficult is its isolation by distillation or sublimation free from traces of H_2SO_4 , if 100% sulfuric acid is used as protonating agent. In general, we can recommend the use of *meta*-phosphoric acid as a nonvolatile protonating reagent superior to sulfuric acid to yield the purest NH acids, such as the known $HNTf_2$, from the corresponding lithium or sodium salts. Conversion of pentafluoroaniline with chlorosulfuric acid and subsequent reaction with phosphorus pentachloride yields $HN(C_6F_5)(SO_2Cl)$.^[23] The chlorine–fluorine exchange is now achieved by potassium fluoride in acetonitrile in the presence of 0.1 equivalents of 18-crown-6, followed by protonation of the generated potassium salt with hydrochloric acid in diethyl ether to yield $HN(Pf)(Sf)$ (Scheme 1).



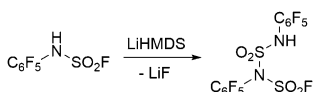
Scheme 1. Syntheses of pentafluorophenyl-substituted NH acids.

For the chemical shifts of the nitrogen acids' acidic protons, a strong solvent dependency is observed in the proton NMR spectra. In the ^{13}C NMR spectra carbon–fluorine coupling is found with typical 1J and 2J coupling constants. The ^{19}F NMR spectra show characteristic chemical shifts for the C_6F_5 moieties and the aliphatic fluorine atoms. The sulfur-bound fluorine atom in $HN(Pf)(Sf)$ exhibits a considerable low-field shift of $\delta =$

54.2 ppm (471 MHz, C_6D_6 , 25 °C). Furthermore, it is worth mentioning that the CF_3 group in $HN(Pf)(Tf)$ shows a coupling through space with the *ortho*-fluorine atoms of the C_6F_5 group with a coupling constant of 5.8 Hz.

Huber et al. reported the preparation of $LiNPf_2$, $LiN(Pf)(Tf)$ and $LiN(Pf)(Nf)$, which show interesting electrochemical properties and are discussed as components in lithium batteries.^[24]

$LiN(Pf)(Hf)$ was prepared in an analogous procedure by the deprotonation of the corresponding NH acid with $LiN(SiMe_3)_2$. In the case of $HN(Pf)(Sf)$, deprotonation led to a nucleophilic attack of the nitrogen atom at the SO_2F moiety of another molecule under formation of lithium fluoride, which can be attributed to the lability of the S–F bond (Scheme 2). The resulting product was characterized via (–)ESI HRMS and XRD analysis (Figure 2).



Scheme 2. Reaction of $HN(Pf)(Sf)$ with $LiN(SiMe_3)_2$.

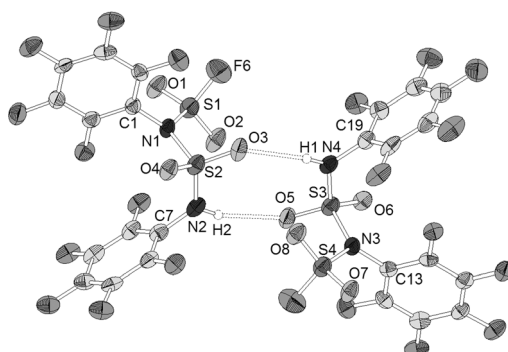


Figure 2. Molecular structure of the dimeric product obtained from the reaction between $HN(Pf)(Sf)$ and $LiN(SiMe_3)_2$ (thermal ellipsoids set at 30% probability).

2.1.2. Structural characterization

In the following section, the molecular structures of the four novel NH acids are described and light is shed on their intermolecular interactions, which are dominated by N–H–O hydrogen-bonds, as well as π–contacts and T-shaped interactions of aromatic groups. Furthermore, molecular structures of the hydrate of $HN(Pf)(Tf)$ and the lithium salt $LiN(Pf)(Nf)$ are presented. Selected bond lengths and angles are summarized in Table 1.

The nitrogen acids reported herein exhibit similar values concerning corresponding bond lengths and angles. C–N dis-

Table 1. Selected bond lengths [pm] and angles [°] found for the molecular structures discussed herein.

	C–N	N–H	O–H	N–S	S–O	S–O	C–N–S
$HN(Pf)(Sf)$	141.8(2)	83(2) ^[a]	227(3) ^[b] 241(2) ^[b]	159.5(2)	140.8(1) ^[c]	141.3(1) ^[c]	120.5(1)
$HN(Pf)(Tf)$	142.1(4)	82(4)	210(4)	159.6(3)	141.6(3)	142.6(2) ^[c]	123.2(2)
$HN(Pf)(Nf)$	142.0(4)	82(2) ^[a]	217(2)	160.5(3)	141.3(2)	142.6(2) ^[c]	125.5(2)
	142.2(4)	84(2) ^[a]	206(2)	160.3(3)	140.9(2)	142.3(2) ^[c]	123.3(2)
$HN(Pf)(Hf)\cdot C_7H_8$	143.3(5)	86(5)	205(5)	161.5(6)	141.6(4)	143.6(4) ^[c]	120.9(3)
$HN(Pf)(Tf)\cdot H_2O$	142.0(4)	185(4)	108(4) ^[d]	153.0(3)	142.7(3) ^[c]	143.5(3) ^[c]	120.3(2)
	143.0(4)	195(4)	109(4) ^[d]	154.8(3)	144.6(3) ^[c]	143.4(2) ^[c]	119.0(2)
$LiN(Pf)(Nf)\cdot 2THF$	139.5(4)	–	–	152.2(3)	143.7(3)	145.0(3)	121.0(2)

[a] N–H bond lengths set during refinement by DFIX command.; [b] the nitrogen atom acts as hydrogen bond donor to the oxygen atoms of two neighboring molecules; [c] oxygen atom acting as hydrogen bond acceptor; [d] O5–H1 and O6–H4.

tances range from 141.8(2) pm ($HN(Pf)(Sf)$) to 143.3(5) pm ($HN(Pf)(Hf)$) and are slightly longer than those in the symmetrical $HNPF_2$ (139.7(3) pm).^[25] The N–S distances lie between 159.5(2) pm ($HN(Pf)(Sf)$) and 161.5(6) pm ($HN(Pf)(Hf)$) and are shorter than observed for the classical acid $HNTf_2$ (N–S 164.4(1) pm).^[26] The S–C bond lengths (184.0(3) pm) in $HNTf_2$ are similar to those for $HN(Pf)(Tf)$ (183.4(4) pm), $HN(Pf)(Nf)$ (184.8(3) pm), and $HN(Pf)(Hf)$ (183.4(7) pm). The same is true for the S–O distances (140.1(2) pm and 141.7(2) pm in $HNTf_2$). As expected, oxygen atoms acting as hydrogen-bond acceptors show slightly longer S–O bond lengths (e.g. 142.6(2) pm in $HN(Pf)(Tf)$) than oxygen atoms that are not involved in hydrogen bonds (e.g. 141.6(3) pm in $HN(Pf)(Tf)$).

HN(Pf)(Sf): Single crystals of $HN(Pf)(Sf)$ were obtained by sublimation at 65 °C and $1.8\cdot 10^{-2}$ mbar. The low steric demand of the SO_2F moiety allows the nitrogen atom to act as a hydrogen bond donor for two oxygen atoms of two vicinal molecules (Figures 3 and 4). Thus, double strands held together by hydrogen bonds and π–interactions of the C_6F_5 moieties are formed. The N–S and the S–F bonds (N1–S1 159.5(2) pm, S1–F6 156.1(1) pm) exhibit similar lengths to those for $HN(C_6H_5)(Sf)$ (N–S 158.7(3) pm, S–F 156.14(19) pm).^[27] The symmetrical $HN(Sf)_2$ has a longer N–S distance (162.7(3) pm) and a shorter S–F bond (153.3(2) pm).^[16b]

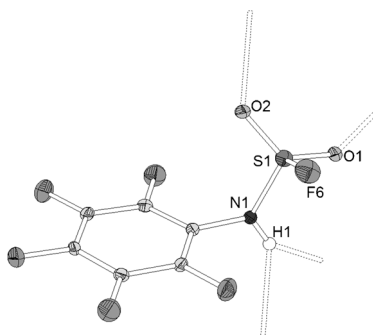


Figure 3. Molecular structure of $HN(Pf)(Sf)$ (thermal ellipsoids set at 30% probability). Selected bond lengths [pm] and angles [°]: C6–N1 141.8(2), N1–S1 159.5(2), S1–O1 140.8(1), S1–O2 141.3(1), S1–F6 156.1(1); C6–N1–S1 120.5(1), O1–S1–O2 123.4(7).

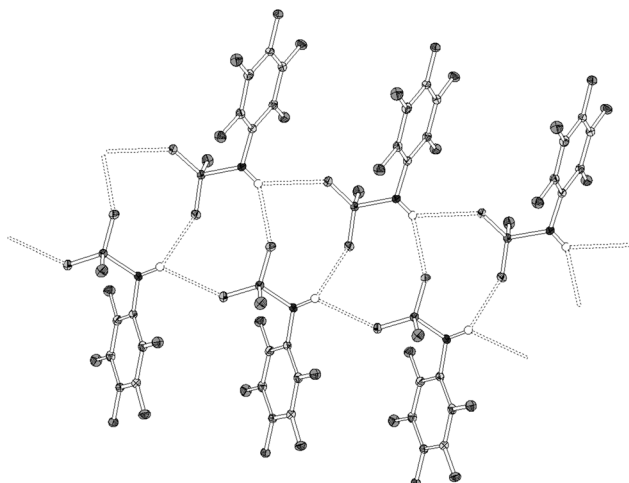


Figure 4. Double strands observed in the solid state structure of $\text{HN}(\text{Pf})(\text{Sf})$.

HN(Pf)(Tf): Single crystals of $\text{HN}(\text{Pf})(\text{Tf})$ were obtained by slow sublimation. In contrast to $\text{HN}(\text{Pf})(\text{Sf})$ no double strands, but only one-dimensional chains connected via N–H–O hydrogen bonds are observed (Figures 5 and 6). Within a chain, the aromatic rings of two neighboring molecules always lie on opposite sides of the chain so that the C_6F_5 moieties are each vicinal to two CF_3 groups. Vicinal chains are linked via T-shaped interactions of pentafluorophenyl groups in a staircase-like manner.

HN(Pf)(Nf): Single crystals of $\text{HN}(\text{Pf})(\text{Nf})$ were obtained by sublimation at 50°C and 5×10^{-2} mbar. The hydrogen-bonding network is similar to that observed for $\text{HN}(\text{Pf})(\text{Tf})$ (Figures 7 and 8). T-shaped interactions between the aromatic rings are evident within the one-dimensional chains.

HN(Pf)(Hf) \cdot C_6H_8 : $\text{HN}(\text{Pf})(\text{Hf})\text{-C}_6\text{H}_8$ was crystallized as colorless needles by cooling a saturated solution in toluene slowly to -30°C . Hydrogen bonds are formed between the nitrogen atom and an oxygen atom of a neighboring $\text{HN}(\text{Pf})(\text{Hf})$ molecule (Figures 9 and 10). On all sides of the chain aromatic rings and alkyl groups alternate, which allows for van der Waals interactions between the C_6F_{17} tails of every second molecule. The asymmetric unit contains one disordered toluene molecule

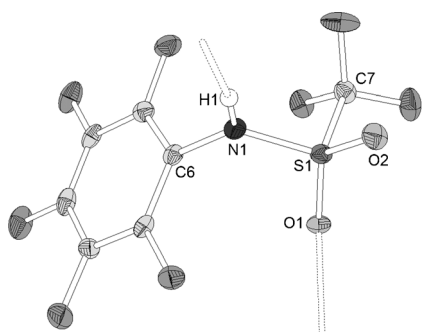


Figure 5. Molecular structure of $\text{HN}(\text{Pf})(\text{Tf})$ (thermal ellipsoids set at 30% probability). Selected bond lengths [pm] and angles [$^\circ$]: C6–N1 142.1(4), N1–S1 159.6(3), S1–O1 142.6(2), S1–O2 141.6(3), S1–C7 183.4(4); C6–N1–S1 123.2(2), O1–S1–O2 122.9(1).

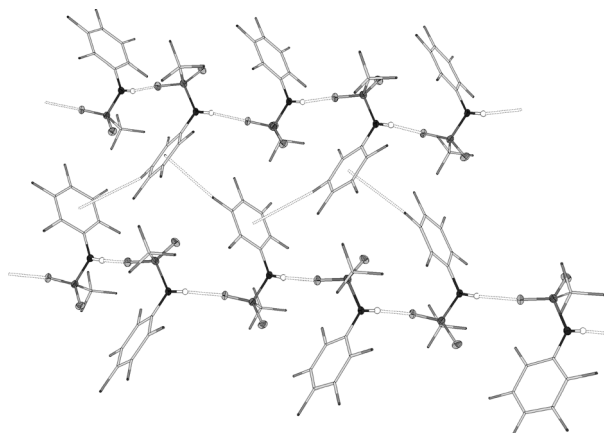


Figure 6. Interactions of one-dimensional $\text{HN}(\text{Pf})(\text{Tf})$ chains via T-shaped interactions of C_6F_5 moieties.

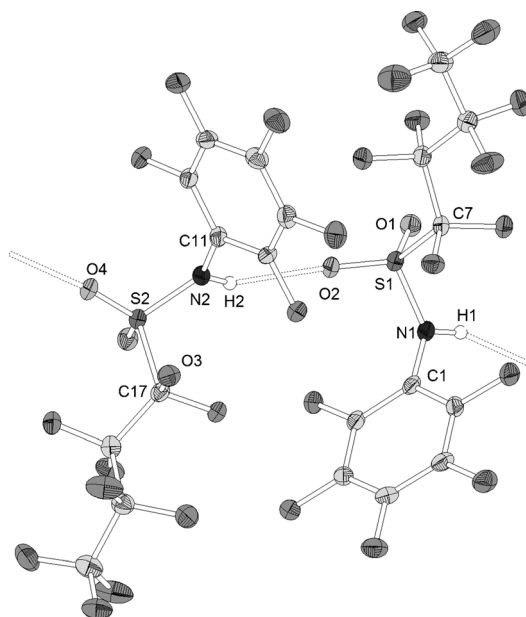


Figure 7. Molecular structure of $\text{HN}(\text{Pf})(\text{Nf})$ (thermal ellipsoids set at 30% probability). Selected bond lengths [pm] and angles [$^\circ$]: C1–N1 142.0(4), N1–S1 160.5(3), S1–O1 141.3(2), S1–O2 142.6(2), S1–C7 184.8(3), C11–N2 142.2(4), N2–S2 160.3(3), S2–O3 140.9(2), S2–O4 142.3(2), S2–C17 184.8(3); C6–N1–S1 125.5(2), O1–S1–O2 122.8(1), C11–N2–S2 123.3(2), O3–S2–O4 123.2(1).

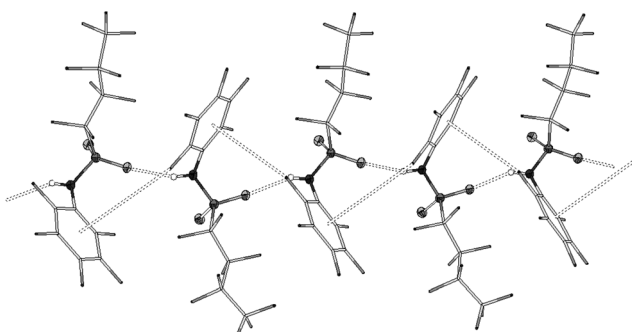


Figure 8. T-shaped interactions between vicinal C_6F_5 moieties within one-dimensional $\text{HN}(\text{Pf})(\text{Nf})$ chains.

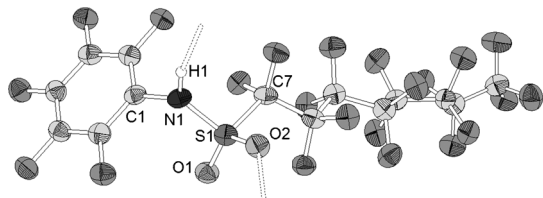


Figure 9. Molecular structure of $\text{HN}(\text{Pf})(\text{Hf}) \cdot \text{C}_7\text{H}_8$ (thermal ellipsoids set at 30% probability; toluene omitted for clarity). Selected bond lengths [pm] and angles [$^\circ$]: C1–N1 143.3(5), N1–S1 161.5(6), S1–O1 141.6(4), S1–O2 143.6(4), S1–C7 183.4(7), C6–N1–S1 120.9(3), O1–S1–O2 122.9(2).

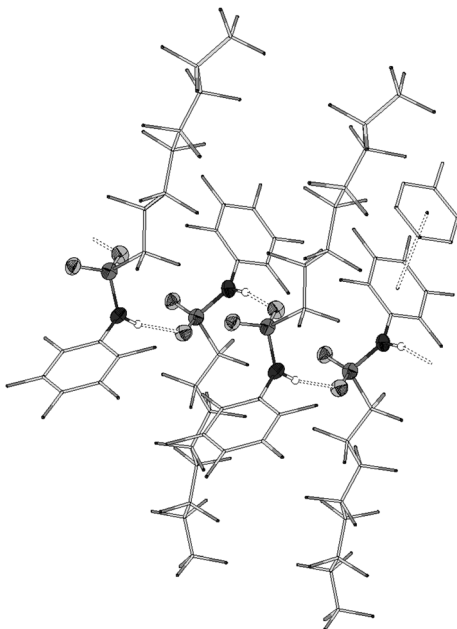


Figure 10. One-dimensional chains in the solid-state structure of $\text{HN}(\text{Pf})(\text{Hf}) \cdot \text{C}_7\text{H}_8$. π -stacking between the toluene molecule and a C_6F_5 ring is observed.

forming π -interactions with a C_6F_5 moiety (angle between C_6F_5 plane and toluene plane: $6.1(2)^\circ$; distances between centroids: 368.54(4) pm and 373.46(4) pm).

HN(Pf)(Tf)·H₂O: The crystal structure suggests that the acidity of the reported compounds is sufficient to protonate water (Figure 11). As observed for the lithium salt of $\text{HN}(\text{Pf})(\text{Nf})$ (see below), the N–S distance in $\text{HN}(\text{Pf})(\text{Tf}) \cdot \text{H}_2\text{O}$ (153.0(3) pm and 154.8(3) pm) is significantly shortened in comparison to the free acid (159.6(3) pm). This emphasizes the high negative partial charge on the oxygen atoms. The water molecules are involved in a complex network of hydrogen bonds. Furthermore, π -contacts between C_6F_5 rings play a role in intermolecular interaction (distance between centroids: 402.8(8) pm, angle between planes of the phenyl rings: 23.4(1) $^\circ$).

LiN(Pf)(Nf)·2THF: Single crystals of $\text{LiN}(\text{Pf})(\text{Nf}) \cdot 2\text{THF}$ were obtained from a solution of $\text{LiN}(\text{Pf})(\text{Nf})$ in THF, revealing a lithium atom coordinated in a distorted tetrahedral fashion by two THF molecules and the oxygen atoms of two neighboring $\text{N}(\text{Pf})(\text{Nf})$ moieties (Figures 12 and 13). One-dimensional chains with the sequence Li–O–S–O with bond angles around the lithi-

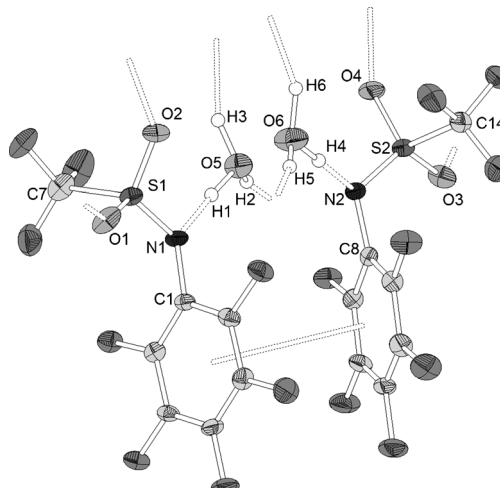


Figure 11. Molecular structure of $\text{HN}(\text{Pf})(\text{Tf}) \cdot \text{H}_2\text{O}$ (thermal ellipsoids set at 30% probability). Selected bond lengths [pm] and angles [$^\circ$]: C1–N1 142.0(4), N1–S1 153.0(3), S1–O1 142.7(3), S1–O2 144.6(3), S1–C7 183.7(4), C8–N2 143.0(4), N2–S2 154.8(3), S2–O3 143.5(3), S2–O4 143.4(2), S2–C14 183.2(3); C6–N1–S1 120.3(2), O1–S1–O2 117.3(2), C8–N2–S2 119.0(2), O3–S2–O4 117.8(1).

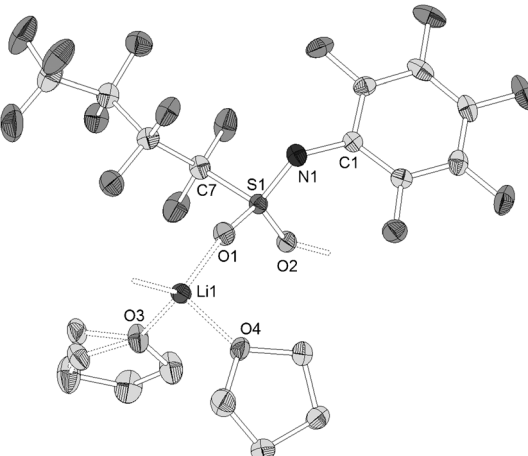


Figure 12. Molecular structure of $\text{LiN}(\text{Pf})(\text{Nf}) \cdot 2\text{THF}$ (thermal ellipsoids set at 30% probability; hydrogen atoms omitted for clarity). Selected bond lengths [pm] and angles [$^\circ$]: C1–N1 139.5(4), N1–S1 152.2(3), S1–O1 143.7(3), S1–O2 145.0(3), S1–C7 185.9(4), Li1–O1 191.6(7), Li1–O2 195.5(7), Li1–O3 192.3(5), Li1–O4 192.7(8), C6–N1–S1 121.0(2), O1–S1–O2 116.0(1), O1–Li1–O2 126.0(3), O1–Li1–O3 105.6(3), O1–Li1–O4 105.8(3), O2–Li1–O3 107.4(3), O2–Li1–O4 106.8(3), O3–Li1–O4 103.1(3).

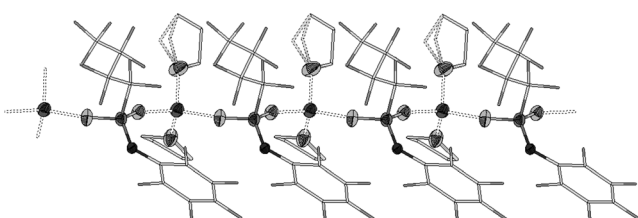


Figure 13. One-dimensional chains formed by $\text{LiN}(\text{Pf})(\text{Nf}) \cdot 2\text{THF}$ (including the disorder of one THF molecule).

um atom ranging from $103.1(3)^\circ$ to $126.0(3)^\circ$ and Li–O distances between $191.6(7)$ pm and $195.5(7)$ pm are formed. Neighboring molecules are oriented with C_4F_9 groups standing at the same side of the chain, allowing for van der Waals interactions. Coordination of the lithium atom by nitrogen atoms or short contacts between the lithium atom and aromatic fluorine atoms are not observed. The N–S distance in the lithium salt ($152.2(3)$ pm) is significantly shorter than those in the free acid ($160.5(3)$ pm and $160.3(3)$ pm), emphasizing a stronger double-bond character. In contrast to the linear chains observed for $\text{LiN}(\text{Pf})(\text{Nf})\cdot 2\text{THF}$, the related lithium salt $\text{LiNPf}_2\cdot \text{THF}$ forms dimers exhibiting short contacts between the lithium atom and two *ortho*-fluorine atoms of vicinal C_6F_5 groups.^[20a]

2.2. Investigation of the acidity of the NH acids

In the following, we analyze the acidity of the new acids in comparison to the known symmetric HNTf_2 and HNPF_2 acids on experimental and computational grounds.

2.2.1. Background to the acidity measurements

Gas-phase acidities: The gas-phase acidity (GA) of an acid H–A is given by its Gibbs energy of dissociation ($\Delta_r G^\circ$) or the gas-phase basicity (GB) of its conjugated base [Eq. (1)]. Strong acids have low GA values. A large collection of GA/GB values that have been obtained by experimental techniques such as FT-ICR-MS and/or quantum chemical procedures is available in the literature.^[2a,28]



We calculated the GA values of the acids HNPF_2 , $\text{HN}(\text{Pf})(\text{Tf})$, $\text{HN}(\text{Pf})(\text{Nf})$, and $\text{HN}(\text{Pf})(\text{Sf})$ using isodesmic proton-exchange reactions based on an initially at the high-level G3_{mod} -calculated^[29] GA value of HNTf_2 .

Calculated pK_a values: In solution, the pK_a value serves as a measure for the acidity of an acid in a given medium. As specified in some recent reviews,^[30] tremendous effort has been made to predict pK_a values computationally, mainly in aqueous solution. Some exemplarily selected examples are given in ref. [31]. In our work, we have focused on calculating pK_a values in DMSO and MeCN solutions.^[28s,32] As a standard for the ab initio pK_a calculations, combinations of high quality GA calculations or experimental values with continuum solvent models^[33] were applied. To improve the obtained results, solvent molecules have to be taken into account explicitly for the dissociation of the acid, for example, in the cluster-continuum model^[31b,34] or the implicit-explicit solvent approach.^[31c] In this study, we employed the recently introduced rCCC model,^[29] coupled with the anchor points^[29] of the newly established unified pH scale,^[35] to predict the pK_a values of the five investigated acids in DMSO and MeCN solutions.

2.2.2. Experimental pK_a values in MeCN

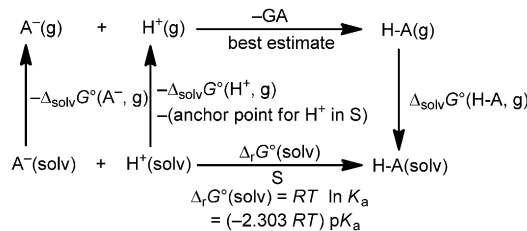
The UV/Vis spectrophotometric titration method used herein was described in detail in ref. [36]. For each investigated compound, the relative acidity and basicity were measured against at least two (mostly three) different reference compounds with known pK_a values in MeCN.^[2c,36] To determine the relative acidity of two compounds, a mixture of two different acids was titrated with UV/Vis radiation non-absorbing acidic (solution of triflic acid in MeCN) and basic (solution of phosphazene $t\text{BuN}=\text{P}(\text{pyrr})_3$ in MeCN) titrants to obtain several spectra of solutions containing both neutral and anionic forms of the two acids in different proportions. Both of the acids were also titrated separately to obtain the spectra of the neutral and anionic forms of the pure compounds. From the titration data, the relative acidity of the acids—the difference between their pK_a values (ΔpK_a)—was calculated.^[36] All of the compounds investigated herein have different spectra of protonated and deprotonated forms in the UV region and calculation methods using only spectral data obtained from the titration of pure compounds and mixture were used to obtain ΔpK_a values. From each titration experiment of the mixture of two compounds, the ΔpK_a value was determined as the mean of 8–20 values. Concentrations of the measured compounds were mostly in the order of $n \times 10^{-5}$ M to $n \times 10^{-4}$ M, whereas concentrations of acidic and basic titrants were in the $n \times 10^{-3}$ M range.

From the ΔpK_a values measured in this work and from the absolute pK_a values assigned to the reference compounds in previous works,^[2c,36] the absolute pK_a values of the investigated compounds were obtained and are presented in Table 2. Also included in Table 2 is the pK_a value of the recently reported hybrid acid $\text{HN}(\text{Pf})\text{C}(\text{CF}_3)_3$.^[37]

2.2.3. Computational Analysis:

Calculation of pK_a values in MeCN and DMSO: Similar to the scheme introduced to determine anchor points^[29] for the Gibbs solvation energies of the proton in DMSO and MeCN (among others), the pK_a values of an acid H–A in DMSO or MeCN solution may be calculated by using the following Born–Fajans–Haber cycle (BFHC 1, Scheme 3; for energy and pK_a values, see Table 4 below):

With the known^[29] anchor points $\Delta_{\text{solv}}G^\circ(\text{H}^+, g \rightarrow S)$ (-1119.6 kJ mol $^{-1}$ for DMSO and -1056.3 kJ mol $^{-1}$ for MeCN), we only had to evaluate the GA values, as well as the Gibbs



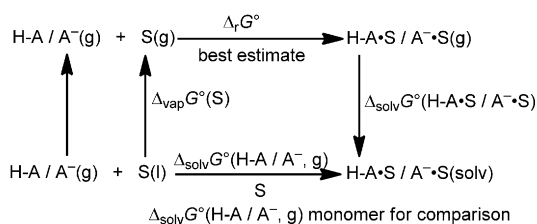
Scheme 3. Born–Fajans–Haber cycle (BFHC 1) for the calculation of the pK_a value of an acid H–A in a solvent S.

Table 2. Results of pK_a measurements in MeCN.

Acid (A)	Reference acid (Ra) ^[a] Identity	pK_a (Ra)	ΔpK_a	pK_a [A]	Assigned pK_a [A]
HNPf ₂	(4-Me-C ₆ F ₄) ₂ CHCN	22.80	-1.17	23.97	23.97
	9-COOMe-fluorene	23.53	-0.44	23.97	
	fluoradene	23.90	-0.06	23.96	
HN(Pf)(Tf)	picric acid	11.00	-0.41	11.41	11.43
	4-H-C ₆ F ₄ CH(CN) ₂	12.98	1.52	11.46	
	(4NC ₅ F ₄) ₂ CHCN	13.46	1.89	11.57	
HN(Pf)(Nf)	4-H-C ₆ F ₄ CH(CN) ₂	12.98	1.81	11.17	11.22
	picric acid	11.00	-0.21	11.21	
	C ₆ (CF ₃) ₄ CH(CN) ₂	10.45	-0.78	11.23	
HN(Pf)(Hf)	picric acid	11.00	-0.21	11.21	11.22
	C ₆ (CF ₃) ₄ CH(CN) ₂	10.45	-0.79	11.24	
	4-H-C ₆ F ₅ CH(CN) ₂	12.98	1.65	11.33	
HN(Pf)C(CF ₃) ₃	9-COOMe-fluorene	23.53	-0.48	24.01	24.01
	fluoradene	23.90	-0.10	24.00	
	C ₆ H ₅ CH(CN)C ₆ F ₅	26.14	2.11	24.03	

[a] pK_a values of the reference acids are from refs. [35] and [38].

solvation energies of the anions A^- and the corresponding acids H–A (Table 4; BFHCs in chapter 4 of the theoretical section of the Supporting Information). We also had to take into account a possible further coordination of solvent molecules to the acids H–A, as well as the corresponding anions A^- . For H–A or for A^- this can be done according to BFHC 2 (Scheme 4) and a subsequent evaluation of their Gibbs solvation energies with the Gibbs solvation energies calculated for the isolated H–A or A^- monomers.



Scheme 4. Born–Fajans–Haber cycle (BFHC) 2 for the calculation of Gibbs solvation energy of an anion A^- or an acid H–A, each coordinated to a solvent molecule S.

For BFHC 2 (Scheme 4), we extracted the Gibbs vaporization energies $\Delta_{vap} G^\circ(S)$ (17.7 kJ mol⁻¹ for DMSO and 5.3 kJ mol⁻¹ for MeCN) from experimental vapor pressures (8×10^{-4} bar for DMSO^[39] and 0.118 bar for MeCN).^[40] The Gibbs gas-phase reaction energies for the coordination of the solvent S to H–A/A⁻ and the Gibbs solvation energies of the aggregates H–A•S/A⁻•S were calculated (see below and the Supporting Information, S-Tables 2 and 3 and BFHCs in chapter 4 of the theoretical section).

Assessment of the GA values: To calculate GAs with good accuracy, we recently established the modified G3 method (G3_{mod}),^[29] which unfortunately is too expensive for the larger

of the here-investigated acids: We barely managed to calculate the GA of HNTf₂ with this method. Therefore, after an extensive method validation with experimental literature GA values (1198.7 kJ mol⁻¹ for HNTf₂^[28] and 1324.2 kJ mol⁻¹ for HNPf₂)^[2a] as a benchmark (chapter 1 of the theoretical section of the Supporting Information), we applied isodesmic reactions as a cheaper alternative to obtain reliable GAs for the acids HN(Pf)(Tf), HN(Pf)(Nf), and HNPf₂ (G3MP2_{mod} → G3_{mod}, see S-Figure 1 in the Supporting Information). For the largest system HN(Pf)(Nf) we had to use the isodesmic approximation twice (M1 → G3MP2_{mod} → G3_{mod} with M1 = MP2(FC)/aug-cc-pVTZ//B3LYP/aug-cc-pVTZ, see the Sup-

porting Information, S-Figure 1), an approach we call isodesmic squared (isodesmic²).

From the results collected in S-Table 1 (see the Supporting Information), we estimate an error bar of around 5–8 kJ mol⁻¹ for the GA values obtained through the isodesmic and isodesmic² approaches and calculated best estimates of the GA from the most acidic HNTf₂ (1197.7 kJ mol⁻¹) over HN(Pf)(Nf) (1251.3 kJ mol⁻¹), HN(Pf)(Tf) (1260.3 kJ mol⁻¹), and HN(Pf)(Sf) (1273.5 kJ mol⁻¹) to the least acidic HNPf₂ (1328.7 kJ mol⁻¹) with our selected reference methods (Table 4).

Gibbs energies of the gas-phase reaction of H–A/A⁻ with MeCN or DMSO: For the determination of the Gibbs gas-phase reaction energies of the coordination of the solvent S to H–A/A⁻, we employed the isodesmic² approach (for H–A = HNPf₂, HN(Pf)(Tf), HN(Pf)(Nf), HN(Pf)(Sf) and A⁻ = N(Pf)(Tf)⁻, N(Pf)(Nf)⁻) or the isodesmic method (for H–A = HNTf₂ and A⁻ = NTf₂⁻, NPF₂⁻). In the special case of A⁻ = N(Pf)(Sf)⁻ we used a directly calculated G3MP2_{mod} value for the coordination of MeCN and an isodesmic² value for the coordination of DMSO (see the Supporting Information; S-Tables 2 and 3, explanations and BFHCs in chapters 2–4 of the theoretical section).

Gibbs solvation energies of acid-solvent (H–A•S) and anion-solvent (A⁻•S) aggregates: We calculated Gibbs solvation energies with COSMO@BP86/def-TZVP for the solvents^[41] MeCN ($\epsilon_r = 36.64$) and DMSO ($\epsilon_r = 46.7$) and compared the values of the recently established vertical or relaxed COSMO cluster-continuum models (vCCC/rCCC).^[29] Vertical and relaxed CCC differ in the inclusion of solvation; with the vCCC model only a single point is done on the gas phase structure, whereas in the rCCC, the gas-phase structure is optimized with COSMO@BP86/def-TZVP in C_1 symmetry.

Ionization of HNTf₂·DMSO: We discovered an amazingly large decrease of the Gibbs solvation energy of HNTf₂·DMSO in DMSO when changing from the vCCC to the rCCC model

$(\Delta_{\text{solv}}G^\circ(\text{rCCC}) - \Delta_{\text{solv}}G^\circ(\text{vCCC}) = -54.5 \text{ kJ mol}^{-1}$). This would be commensurate to an increase of $-54.5/5.71 = 9.5 \text{ p}K_a$ units upon changing from vertical to relaxed structures ($\Delta \text{p}K_a = 1$ corresponds to $RT \ln 0.1 = -5.71 \text{ kJ mol}^{-1}$ at 298.15 K),^[29,35] neglecting the small energy differences between the vCCC and the rCCC model at other parts of the BFHCs. Looking at the respective structures reveals what to our knowledge is a hitherto-unencountered phenomenon: The DMSO adduct of HNTf₂ ionizes during optimization with COSMO@BP86/def-TZVP by transfer of the proton from N to O, yielding a contact ion pair. Thus, $d(\text{N}-\text{H})$ is elongated from 110.0 pm (vCCC) to 157.9 pm (rCCC) and $d(\text{H}-\text{O})$ is shortened from 151.7 pm (vCCC) to 104.9 pm (rCCC) (Figure 14).

Table 3. Bond lengths of the hydrogen bond of the acid-solvent adducts optimized in the gas phase (vCCC model) and in solution (rCCC model). Changes of the Gibbs solvation energies from vCCC to rCCC.

Investigated species	(Acid)N–H bond		H–NCMe bond		vCCC → rCCC	
	vCCC [pm]	rCCC [pm]	vCCC [pm]	rCCC [pm]	$\Delta(\Delta_{\text{solv}}G^\circ)$ [kJ mol ⁻¹]	
MeCN adducts	HNTf ₂ ·MeCN	105.2	107.2	181.9	169.8	-4.6
	HNPF ₂ ·MeCN	103.1	103.5	198.8	194.2	-0.6
	HN(Pf)(Tf)·MeCN	104.0	105.0	190.3	181.3	-4.6
	HN(Pf)(Nf)·MeCN	103.8	105.0	191.2	181.7	-4.5
	HN(Pf)(Sf)·MeCN	104.2	105.5	188.6	178.8	-5.6
DMSO adducts	(Acid)N–H bond		H–O(DMSO) bond		vCCC → rCCC	
	vCCC [pm]	rCCC [pm]	vCCC [pm]	rCCC [pm]	$\Delta(\Delta_{\text{solv}}G^\circ)$ [kJ mol ⁻¹]	
			110.0	157.9	-54.5	
			104.4	105.4	-4.2	
			106.7	109.9	-12.9	
	HN(Pf)(Nf)·DMSO		106.9	110.5	-15.0	
	HN(Pf)(Sf)·DMSO		106.9	111.3	-20.0	

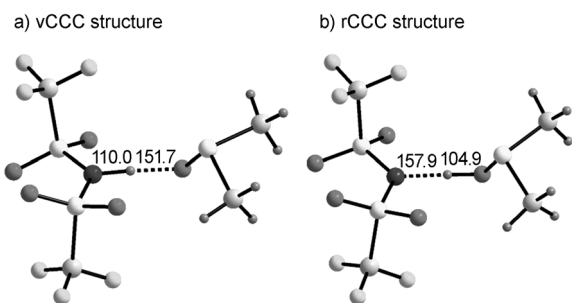


Figure 14. Calculated structures of the DMSO solvates of the HNTf₂ acid optimized in the gas phase (a) and in DMSO solution (b). Distances in pm. Note the transfer of the proton from the N to the O (DMSO) atom upon inclusion of solvation.

To rule out attribution of the phenomenon solely to an influence of the functional or the basis set, we also employed COSMO@B3LYP/aug-cc-pVTZ. The observed effect is even larger here with an energy decrease of $-68.1 \text{ kJ mol}^{-1}$ from vCCC to rCCC, a corresponding elongation of $d(\text{N}-\text{H})$ from 106.9 pm (vCCC) to 170.0 pm (rCCC) and a shortening of $d(\text{H}-\text{O})$ from 158.5 pm (vCCC) to 100.9 pm (rCCC). To eliminate also the possibility of a COSMO artifact, we transferred the vCCC and rCCC methodology to the polarizable continuum model (PCM) by performing a PCM@BP86/TZVP single point in DMSO based on the BP86/def-TZVP-optimized gas-phase structure of HNTf₂·DMSO and a PCM@BP86/TZVP full optimization in DMSO. The obtained results confirm our previous studies accompanied by an energy decrease during optimization of $-41.9 \text{ kJ mol}^{-1}$ and an optimized structure with 154.7 pm for $d(\text{N}-\text{H})$ and 106.1 pm for $d(\text{H}-\text{O})$. Thus, the magnitude of the effect is similar to that for COSMO.

Investigation of other H–A–S solvates: We then decided to systematically examine the behavior of the MeCN and DMSO adducts of all the investigated acids upon optimization with COSMO (Table 3). For the adducts of the more basic DMSO solvent we found a more pronounced trend towards “ionization” during optimization that led to a larger decrease of the Gibbs solvation energies from the vCCC to the rCCC model, and from HNPf₂ over HN(Pf)(Tf), HN(Pf)(Nf) and HN(Pf)(Sf) to HNTf₂. This order also corresponds to increased acidity according to the GA values of the respective acids with HN(Pf)(Sf) as an anomaly.

Some words of caution have to be mentioned. Apart from HNTf₂·DMSO the developing ionization does not lead to real contact ion pairs. However, there are significant energetic and structural changes. For HN(Pf)(Sf)·DMSO the change of the N–H/H–O bonds from vCCC to rCCC amounts to +4.4/−15.5 pm and the change of the Gibbs solvation energy value to $-20.0 \text{ kJ mol}^{-1}$. Similar values were calculated for HN(Pf)(Nf)·DMSO (N–H/H–O change: +3.6/−13.5 pm; energy change: $-15.0 \text{ kJ mol}^{-1}$) and HN(Pf)(Tf)·DMSO (+3.2/−11.8 pm and $-12.9 \text{ kJ mol}^{-1}$). The smallest alterations were for the DMSO adduct of the weakest acid HNPf₂ (+1.0/−6.4 pm and -4.2 kJ mol^{-1}). For the adducts of the acids and the much less basic solvent MeCN, the “ionization” effect was only marginal, with overall small elongations of the (acid) N–H bond and a small decrease of the Gibbs solvation energy values, but a relatively large shortening of the H–NCMe bond (from -4.6 pm at HNPf₂·MeCN to -12.1 pm at HNTf₂·MeCN). The structural and energetic changes are collected in Table 3.

Investigation of the A[−]·S solvates: When assessing the Gibbs solvation energies of the anion–solvent aggregates A[−]·S, switching from the vCCC to the rCCC model, a slight structural relaxation in the rCCC model is accompanied by changes of the Gibbs solvation energies that were in this case larger for the MeCN adducts than for the DMSO adducts (up to $-17.2 \text{ kJ mol}^{-1}$ for N(Pf)(Tf)[−]·MeCN; see BFHCs in chapter 4 of the theoretical section of the Supporting Information).

2.3. Discussion of the gas-phase and solution acidity of the investigated acids

Our measured and calculated (rCCC) pK_a values are collected in Table 4. The calculated values differ by at most 3.1 pK_a units from the experimental values. This is within our estimated error bar of 20 kJ mol⁻¹ (20/5.71 = 3.5 pK_a units), and mainly due to the residual error of the rCCC Gibbs solvation energies.

Table 4. pK_a values based on the rCCC model (bold type, vCCC values in brackets for comparison) of the five investigated acids in MeCN and DMSO as well as GA values [in kJ mol⁻¹] and all rCCC Gibbs solvation energies [kJ mol⁻¹] (known anchor points for H⁺, taken from Scheme 4 for H-A, A⁻) needed to calculate these pK_a values using Scheme 3. Experimental pK_a and GA values, if available.

Acidity	HNTf ₂	HNPF ₂	HN(Pf)(Tf)	HN(Pf)(Nf)	HN(Pf)(Sf)
GA (exp.)	1198.7 ^[28]	1324.2 ^[2a]			
GA (best estimate)	1197.7	1328.7	1260.3	1251.3	1273.5
Solvation with MeCN					
$\Delta_{\text{solv}}G^\circ(\text{H}^+, \text{g})$ (rCCC)	-1056.3	-1056.3	-1056.3	-1056.3	-1056.3
$\Delta_{\text{solv}}G^\circ(\text{H}-\text{A}, \text{g})$ (rCCC)	-60.2	-35.6	-63.3	-63.6	-56.6
$\Delta_{\text{solv}}G^\circ(\text{A}^-, \text{g})$ (rCCC)	-216.9	-174.0	-211.8	-202.7	-223.9
pK_a MeCN (rCCC)	-2.7	23.5	9.7	9.8	8.7
pK_a MeCN (exp.)	0.3 ^[2c]	23.97	11.43	11.22	-
[pK_a MeCN (vCCC)]	[0.5]	[26.1]	[13.2]	[13.1]	[11.9]
Solvation with DMSO					
$\Delta_{\text{solv}}G^\circ(\text{H}^+, \text{g})$ (rCCC)	-1119.6	-1119.6	-1119.6	-1119.6	-1119.6
$\Delta_{\text{solv}}G^\circ(\text{H}-\text{A}, \text{g})$ (rCCC)	-130.0	-54.2	-76.8	-78.6	-80.1
$\Delta_{\text{solv}}G^\circ(\text{A}^-, \text{g})$ (rCCC)	-214.3	-180.6	-209.8	-201.1	-224.9
pK_a DMSO (rCCC)	-1.1	14.5	1.3	1.6	1.6
pK_a DMSO (exp.)	2.0 ^[42]	12.6^[43]	-	-	-
[pK_a DMSO (vCCC)]	[−8.8]	[15.7]	[1.0]	[0.9]	[0.3]

vCCC values lack structural relaxation in their solvation Gibbs energy and are only given for comparison in Table 4, but should not be used. The trends of the pK_a values in MeCN and DMSO show a similar sequence to the GA values, but for HN(Pf)(Tf), HN(Pf)(Nf), and HN(Pf)(Sf)—although their GA values scatter over a range of 22.2 kJ mol⁻¹ (22.2/5.71 = 3.9 pK_a units)—nearly the same rCCC pK_a values in DMSO occur due to variations in Gibbs solvation energies of HN(Pf)(Tf)/(Pf)(Tf)⁻ and of the corresponding solvent aggregates (Scheme 4), compared to HN(Pf)(Nf)/(Pf)(Nf)⁻ and/or HN(Pf)(Sf)/(Pf)(Sf)⁻. Thus, the weakest asymmetric acid in the gas phase—HN(Pf)(Sf)—is in MeCN the most acidic of the three mixed acids HN(Pf)(Tf), HN(Pf)(Nf), and HN(Pf)(Sf) according to the calculations. HNPF₂ is expectedly the weakest acid in the series and is almost exactly as acidic as HN(Pf)C(CF₃)₃. Thus, in the context of acidifying effect, C₆F₅ and C(CF₃)₃ behave in a very similar way, although they have quite different steric demands.

For HNTf₂, a significant anomaly appeared, mainly due to the effect of contact ion pair formation in DMSO: The rCCC pK_a value in MeCN is lower than in DMSO due to the increase of pK_a value by 7.7 pK_a units^[44] from the vCCC to the rCCC value in DMSO. The reason is that in the course of rCCC geometry optimization, proton transfer occurs within the species Me₂SO···HNTf₂, to give Me₂SO-H⁺···NTf₂⁻. Using the latter species as the neutral acidic form leads to grossly underestimated

acidity (overestimated pK_a value), because our initial state is not the neutral HNTf₂ molecule any more but the ion pair, in which HNTf₂ is in fact already deprotonated. In other words, the rCCC pK_a value in DMSO is rather the dissociation constant of the contact ion pair than the acidity constant of HNTf₂.

This is also supported by observing the rCCC acidity change in the hypothetical row of transformations HNPF₂→HN(Pf)(Tf)→HNTf₂. In MeCN the pK_a changes corresponding to the two steps are around -14 and -12 pK_a units, respectively; in DMSO, however, the changes are -13 and -2.4. Given the generally very good correlation between pK_a values in MeCN and DMSO, it is difficult to see why the trends in this row of changes should be so different between the two solvents.

Interestingly, the rCCC pK_a of HNTf₂ in DMSO is in agreement with the experimentally determined acidity. There is, however, strong reason to believe that the experimental pK_a value of HNTf₂ in DMSO of 2.0 is several orders of magnitude too high for the pK_a of "molecular" HNTf₂. This value has been obtained using potentiometric titration and the actual presence of the molecule HNTf₂ in solution was not monitored in any way. The dangers of

pK_a determination of strong acids in DMSO, whereby the protonated form of the acid is actually not monitored in the solution, were discussed in a recent paper.^[45] Thus, we conclude it was actually the Me₂SO-H⁺···NTf₂⁻ contact ion pair that was titrated.

Such contact ion pair formation in DMSO solution may also explain observations reported by Kütt et al.^[36] When they plotted pK_a values in MeCN against pK_a values in DMSO, there were two significant outliers, namely the strong acids 4-Me-C₆H₄SO₃H and C₆H₅CH(SO₂CF₃)₂, with deviations of -4.6 and -6.4 pK_a units in MeCN, respectively.

The vCCC pK_a value of HNTf₂, however, fits very well with the above-discussed trend of acidity change from HNPF₂ to HNTf₂. Indeed this vCCC pK_a can be interpreted as the pK_a of a "HNTf₂ molecule in DMSO".^[46] However, as this pK_a value exists only in silico, and has not been experimentally observed in real DMSO, this pK_a value is a hypothetical one.

Overall, we found a much lower range of acidities in DMSO than in MeCN. Similar to the difference of the absolute acidities at equal pH in MeCN and DMSO of 11.1 pH_{abs} units ($\Delta(\Delta_{\text{solv}}G^\circ(\text{H}^+ \text{ in S})$: -1056.3 + 1119.6 = 63.3 kJ mol⁻¹; in logarithmic units: 63.3/5.71 = 11.1 pH_{abs} units), the difference between the pK_a values in MeCN and DMSO at the rCCC level is 9.0 for HNPF₂ and decreases through HN(Pf)(Tf) (8.4), HN(Pf)(Nf) (8.2), and HN(Pf)(Sf) (7.1), to HNTf₂ (-1.6, with full formation of

a contact ion pair in DMSO). This is mainly attributed to the increase of contact ion pair formation in DMSO. Our computations and the above reasoning provide strong evidence that the anomalously high experimental DMSO pK_a value of Tf_2NH (and possibly other strong acids, such as TfOH) is in fact the dissociation constant of a contact ion pair.

3. Conclusion/Outlook

We described a family of perfluorinated sulfonylanilides with a tunable acidity and lipophilicity depending on the length of the perfluoroalkyl chain. Due to the asymmetric nature of their anions, their anion polarizabilities and ligand properties differ from those of the parent symmetric NH acids HNTf_2 and HNPF_2 . This opens new perspectives in the design of thermally stable Lewis acids with weakly coordinating anions or thermally stable lithium electrolytes and ionic liquids with tunable anion properties.

The gas-phase and solution acidities of these NH acids were determined experimentally in MeCN, and computationally in the gas phase, as well as in MeCN and DMSO solution. Experimental and calculated values generally agreed well, with the exception of the interesting HNTf_2 /DMSO case: In this case we encountered the transition from molecular to medium acidity when changing from the vertical (vCCC) to the relaxed (rCCC) model. That means with the vertical model, including the gas-phase structure of the DMSO adduct of HNTf_2 , we still describe the—attenuated—acidity of the molecular acid HNTf_2 . If we allow structural relaxation during the optimization of the solvated adduct, a proton transfer occurs and now, in the rCCC model, we describe the molecular acidity of protonated DMSO solvated by the NTf_2^- anion. This proton transfer signals that HNTf_2 in DMSO medium is a strong acid that allows solvent protonation. However, it implies that our rCCC-calculated pK_a value of HNTf_2 in DMSO is not the pK_a of HNTf_2 but that of $\text{H}-\text{DMSO}^+[\text{NTf}_2^-]$ in DMSO.

4. Experimental Section

All reactions were carried out under an inert atmosphere using standard Schlenk techniques. Moisture and air sensitive substances were stored in a conventional nitrogen-flushed glovebox. Solvents were purified according to literature procedures and kept under an inert atmosphere. Pentafluoroaniline (Chempur), triflic acid anhydride (Chempur), nonafluorobutylsulfonylfluoride (Aldrich), and heptadecaoctylsulfonylfluoride (Chempur) were purchased from commercial sources. Sodium bis(trimethylsilyl)amide,^[47] lithium bis(trimethylsilyl)amide^[47] and $\text{HN}(\text{C}_6\text{F}_5)(\text{SO}_2\text{Cl})^{[23]}$ were prepared according to literature procedures.

Spectra were recorded on the following spectrometers: NMR: Bruker ARX300, Bruker DRX400, Bruker DRX500; IR: ATR-FT-IR; MS: LTQ-FT or QStarPulsari (Finnigan); elemental analysis: CHN-Rapid (Heraeus).

Synthesis and characterization

HN(Pf)(Tf): A solution of 2,3,4,5,6-pentafluoroaniline (8.86 g, 48.34 mmol) in diethyl ether (20 mL) was added to a solution of sodium bis(trimethylsilyl)amide (17.75 g, 96.80 mmol) in diethyl

ether (100 mL) at -78°C . The resulting solution was brought to 0°C and stirred at this temperature for 2 h. The reaction mixture was cooled again to -78°C and a precooled solution of triflic acid anhydride (8.14 mL, 48.34 mmol) in diethyl ether (50 mL) was added slowly to the reaction mixture via a cannula. The reaction mixture was slowly brought to room temperature and stirred for 12 h. All volatiles were removed in vacuo at 50°C . The colorless residue was suspended in CFCl_3 (100 mL) and the suspension was cooled to 0°C . Concentrated sulfuric acid (15 mL) was then added and the mixture was heated at reflux for two additional hours. The phases were separated by decantation and the fluorous phase was stored at -30°C , which lead to the formation of colorless crystals. The precipitate was separated from the solution, dried in vacuo, and finally sublimed (90°C , 1.0×10^{-2} mbar). This gave $\text{HN}(\text{Pf})(\text{Tf})$ (10.45 g, 69%) as a colorless solid. M.p. 56°C ; ^1H NMR (300 MHz, $[\text{D}_6]\text{DMSO}$, 25°C , TMS): $\delta = 12.33$ ppm (s, 1 H, NH); ^{13}C NMR (101 MHz, CDCl_3 , 25°C , TMS): $\delta = 146.6$ – 143.8 (m, $^1\text{J}(\text{C},\text{F}) = 252.3$ Hz, CF_{Ar}), 144.1 – 141.1 (m, $^1\text{J}(\text{C},\text{F}) = 265.4$ Hz, CF_{Ar}), 139.3 – 136.5 (m, $^1\text{J}(\text{C},\text{F}) = 254.4$ Hz, CF_{Ar}), 119.3 (q, $^1\text{J}(\text{C},\text{F}) = 321.3$ Hz, CF_3), 108.2 ppm (t, $^2\text{J}(\text{C},\text{F}) = 17.1$ Hz, *ipso*-C); ^{19}F NMR (346 MHz, CDCl_3 , 25°C , CFCl_3): $\delta = -77.0$ (t, $^{19}\text{J}(\text{F},\text{F}) = 5.8$ Hz, 3 F, CF_3), -142.9 (d, $^3\text{J}(\text{F},\text{F}) = 22.6$ Hz, 2 F, o-F), -149.7 (t, $^3\text{J}(\text{F},\text{F}) = 21.4$ Hz, 1 F, p-F), -160.1 ppm (t, $^3\text{J}(\text{F},\text{F}) = 18.6$ Hz 2 F, m-F); IR (Nujol): $\nu = 631$ (m), 681 (w), 895 (s), 986 (s), 1047 (s), 1119 (s), 1140 (w), 1159 (w), 1180 (s), 1205 (s), 1287 (s), 1317 (m), 1502 (m), 1520 (m), 1649 (w), 3219 cm^{-1} (br, NH); MS (70 eV): m/z (%): 315 (8) [M^+], 182 (92) [HNC_6F_5^+], 155 (51) [C_5F_5^+], 69 (100) [CF_3^+]; elemental analysis calcd (%) for $\text{C}_7\text{HF}_8\text{NO}_2\text{S}$: C 26.68, H 0.32, N 4.44; found: C 26.21, H 0.57, N 4.37.

HN(Pf)(Nf): A solution of 2,3,4,5,6-pentafluoroaniline (8.56 g, 46.77 mmol) in diethyl ether (20 mL) was added to a solution of sodium bis(trimethylsilyl)amide (17.15 g, 93.53 mmol) in diethyl ether (100 mL) at -78°C . The resulting solution was brought to 0°C and stirred at this temperature for 2 h. The reaction mixture was cooled again to -78°C and a precooled solution of nonafluorobutylsulfonylfluoride (8.40 mL, 46.77 mmol) in diethyl ether (50 mL) was added slowly to the reaction mixture via a cannula. The reaction mixture was slowly brought to room temperature and stirred for 12 h. All volatiles were removed in vacuo at 50°C . The colorless residue was suspended in CFCl_3 (100 mL) and the suspension was cooled to 0°C . Then concentrated sulfuric acid (15 mL) was added and the mixture was heated at reflux for two additional hours. The phases were separated by decantation and the fluorous phase was evaporated to dryness in vacuo. The residue was sublimed (100°C , 1.0×10^{-2} mbar) to yield $\text{HN}(\text{Pf})(\text{Nf})$ (18.18 g, 84%) as a colorless solid. M.p. 73°C ; ^1H NMR (300 MHz, $[\text{D}_6]\text{DMSO}$, 25°C , TMS): $\delta = 13.24$ ppm (s, 1 H, NH); ^{13}C NMR (101 MHz, CDCl_3 , 25°C , TMS): $\delta = 146.5$ – 143.7 (m, $^1\text{J}(\text{C},\text{F}) = 255.2$ Hz, CF_{Ar}), 144.1 – 141.3 (m, $^1\text{J}(\text{C},\text{F}) = 261.1$ Hz, CF_{Ar}), 139.4 – 136.5 (m, $^1\text{J}(\text{C},\text{F}) = 254.3$ Hz, CF_{Ar}), 117.1 (tq, $^1\text{J}(\text{C},\text{F}) = 288.4$ Hz, $^2\text{J}(\text{C},\text{F}) = 32.9$ Hz, CF_3), 114.9 (tt, $^1\text{J}(\text{C},\text{F}) = 300.4$ Hz, $^2\text{J}(\text{C},\text{F}) = 35.5$ Hz, $-CF_2-$), 110.2 (tt, $^1\text{J}(\text{C},\text{F}) = 270.0$ Hz, $^2\text{J}(\text{C},\text{F}) = 31.6$ Hz, $-CF_2-$), 108.5 (t, $^2\text{J}(\text{C},\text{F}) = 14.9$ Hz, *ipso*-C), 108.3 ppm (tt, $^1\text{J}(\text{C},\text{F}) = 270.5$ Hz, $^2\text{J}(\text{C},\text{F}) = 33.1$ Hz, $-CF_2-$); ^{19}F NMR (376 MHz, CDCl_3 , 25°C , CFCl_3): $\delta = -81.1$ (t, $^3\text{J}(\text{F},\text{F}) = 9.8$ Hz, 3 F, CF_3), -111.6 – -111.4 (m, 2 F, $-CF_2-\text{CF}_3$), -121.1 (br s, 2 F, $-CF_2-$), -126.2 – -126.4 (m, 2 F, $-\text{SO}_2-\text{CF}_2$), -142.7 – -142.9 (m, 2 F, o-F), -150.1 (t, $^3\text{J}(\text{F},\text{F}) = 21.4$ Hz, 1 F, p-F), -160.5 – -160.7 ppm (m, 2 F, m-F); IR (Nujol): $\nu = 625$ (m), 650 (m), 681 (w), 700 (w), 735 (m), 833 (w), 893 (s), 991 (s), 1053 (m), 1136 (s), 1209 (s), 1518 (m), 1629 (w), 3270 cm^{-1} (br, NH); MS (70 eV): m/z (%): 465 (8) [M^+], 232 (8) [M^{2+}], 182 (100) [HNC_6F_5^+], 155 (30) [C_5F_5^+], 69 (52) [CF_3^+]; elemental analysis calcd (%) for $\text{C}_{11}\text{HF}_{14}\text{NO}_2\text{S}$: C 25.82, H 0.22, N 3.01; found: C 25.62, H 0.28, N 3.17.

HN(Pf)(Hf): A solution of 2,3,4,5,6-pentafluoroaniline (4.47 g, 24.4 mmol) in diethyl ether (20 mL) was added to a solution of sodium bis(trimethylsilyl)amide (4.47 g, 24.4 mmol) in diethyl ether (50 mL) at -78°C . The resulting solution was brought to 0°C and stirred at this temperature for 2 h. The reaction mixture was cooled again to -78°C and a precooled solution of heptadecaoctylsulfanylfluoride (6.6 mL, 24.4 mmol) in diethyl ether (25 mL) was added slowly. The reaction mixture was brought to room temperature overnight and all volatiles were removed in vacuo. The brown residue was treated with a mixture of metaphosphoric acid and phosphorous pentoxide (1:1 *m/m*; 6 mL) and sublimed from the viscous mixture (140°C , 1.0×10^{-2} mbar) to yield HN(Pf)(Hf) (7.17 g, 43%) as an off-white solid. M.p. 90°C ; ^1H NMR (400 MHz, $[\text{D}_6]\text{DMSO}$, 25°C , TMS): $\delta = 14.16$ ppm (s, 1 H, NH); ^{13}C NMR (101 MHz, C_6D_6 , 25°C , TMS): $\delta = 145.0$ ppm (pd, $^1\text{J}(\text{C},\text{F}) = 254.9$ Hz, CF_{Ar}), 142.2 (pd, $^1\text{J}(\text{C},\text{F}) = 251.5$ Hz, $p\text{-C}_{\text{Ar}}$), 137.7 (pd, $^1\text{J}(\text{C},\text{F}) = 251.2$ Hz, CF_{Ar}), 117.5 (qt, $^1\text{J}(\text{C},\text{F}) = 288.5$ Hz, $^2\text{J}(\text{C},\text{F}) = 32.9$ Hz, CF_3), 115.4 (tt, $^1\text{J}(\text{C},\text{F}) = 300.4$ Hz, $^2\text{J}(\text{C},\text{F}) = 35.2$ Hz, SO_2CF_2), 114.5–107.9 ppm (m, $\text{CF}_2 + ipso\text{-C}_{\text{Ar}}$); ^{19}F NMR (376 MHz, $[\text{D}_6]\text{DMSO}$, 25°C , FCCl_3): $\delta = -79.6$ – -79.4 (m, 3 F, CF_3), -113.2 – -112.9 (m, 2 F, CF_2), -119.1 (br s, 2 F, CF_2), -121.1 – -120.6 (m, 6 F, CF_2), -121.7 (br s, 2 F, CF_2), -125.1 – -124.9 (m, 2 F, CF_2), -148.8 – -148.6 (m, 2 F, $o\text{-F}_{\text{Ar}}$), -165.9 – -165.6 (m, 2 F, $m\text{-F}_{\text{Ar}}$), -166.6 – -166.2 ppm (m, 1 F, $p\text{-F}$); IR: $\tilde{\nu} = 444$ (m), 481 (m), 516 (m), 549 (m), 601 (m), 618 (m), 657 (w), 694 (w), 738 (w), 747 (w), 852 (w), 888 (w), 992 (s), 1038 (m), 1125 (m), 1149 (s), 1187 (m), 1215 (m), 1370 (m), 1434 (m), 1516 (s), 3233 cm^{-1} (w, NH); (–)ESI-MS (CH_2Cl_2): m/z (%): 664 (100) [$M-\text{H}^+$], 181 (23) [$M-\text{SO}_2\text{C}_8\text{F}_{17}$]; HRMS ((–)ESI (CH_2Cl_2)): m/z calcd for $\text{C}_{14}\text{F}_{22}\text{NO}_2\text{S}^-$ 663.9304 [$M-\text{H}^+$]; found: 663.9293; elemental analysis calcd (%) for $\text{C}_{14}\text{HF}_{22}\text{NO}_2\text{S}$: C 25.28, H 0.15, N 2.11, S 4.82; found: C 25.12, H 0.22, N 2.35, S 4.97.

LiN(Pf)(Hf): A solution of lithium bis(trimethylsilyl)amide (75 mg, 0.451 mmol) in toluene (5 mL) was added dropwise to a solution of $\text{HN}(\text{C}_6\text{F}_5)(\text{SO}_2\text{C}_8\text{F}_{17})$ (300 mg, 0.451 mmol) in toluene (10 mL). Immediately a white solid precipitated. After stirring the suspension for 2 h at room temperature the precipitate was separated by centrifugation, washed with hexane (2×15 mL) and dried in vacuo. LiN(Pf)(Hf) (258 mg, 85%) was obtained as an off-white solid. ^{13}C NMR (101 MHz, $[\text{D}_6]\text{DMSO}$, 25°C , TMS): $\delta = 142.9$ (pd, $^1\text{J}(\text{C},\text{F}) = 240.1$ Hz, CF_{Ar}), 136.9 (pd, $^1\text{J}(\text{C},\text{F}) = 244.1$ Hz, CF_{Ar}), 134.8 (pd, $^1\text{J}(\text{C},\text{F}) = 241.6$ Hz, $p\text{-C}_{\text{Ar}}$), 123.4 (t, $^2\text{J}(\text{C},\text{F}) = 15.2$ Hz, $ipso\text{-C}_{\text{Ar}}$), 116.5 (qt, $^1\text{J}(\text{C},\text{F}) = 288.4$ Hz, $^2\text{J}(\text{C},\text{F}) = 33.3$ Hz, CF_3), 115.0 (tt, $^1\text{J}(\text{C},\text{F}) = 293.6$ Hz, $^2\text{J}(\text{C},\text{F}) = 32.8$ Hz, SO_2CF_2), 109.6 (tt, $^1\text{J}(\text{C},\text{F}) = 239.9$ Hz, $^2\text{J}(\text{C},\text{F}) = 31.4$ Hz, CF_2), 113.9–106.9 ppm (m, CF_2); ^{19}F NMR (376 MHz, $[\text{D}_6]\text{DMSO}$, 25°C , FCCl_3): $\delta = -80.0$ (t, $^3\text{J}(\text{F},\text{F}) = 9.7$ Hz, 3 F, $-\text{CF}_3$), -113.5 (s, 2 F, $-\text{CF}_2-$), -119.4 (s, $-\text{CF}_2-$), -121.2 – -121.4 (m, 6 F, $-\text{CF}_2-$), -122.1 (s, 2 F, $-\text{CF}_2-$), -125.4 (br s, 2 F, $-\text{CF}_2-$), -149.4 (d, $^3\text{J}(\text{F},\text{F}) = 24.7$ Hz, 2 F, $o\text{-F}$), -166.6 (t, $^3\text{J}(\text{F},\text{F}) = 21.6$ Hz, 2 F, $m\text{-F}$), -168.1 ppm (t, $^3\text{J}(\text{F},\text{F}) = 22.7$ Hz, 1 F, $p\text{-F}$); IR: $\tilde{\nu} = 415$ (w), 527 (m), 552 (m), 602 (w), 631 (m), 660 (w), 680 (w), 708 (w), 745 (w), 815 (w), 850 (w), 898 (m), 985 (s), 1061 (m), 1140 (s), 1199 (s), 1274 (m), 1320 (w), 1369 (w), 1465 (w), 1502 (m), 1521 (m), 1654 (w), 2979 cm^{-1} (w); (–)ESI-MS (MeCN): m/z (%): 664 (100) [M]; HRMS ((–)ESI (MeCN)): m/z calcd for $\text{C}_{14}\text{F}_{22}\text{NO}_2\text{S}^-$ 663.9304 [M^-]; found: 663.9295; elemental analysis calcd (%) for $\text{C}_{14}\text{F}_{22}\text{LiNO}_2\text{S}$: C 25.05, H 0.00, N 2.09, S 4.78; found: C 25.81, H 0.48, N 2.56, S 4.32.

HN(Pf)(Sf): A mixture of *H-N*(2,3,4,5,6-pentafluorophenyl)-sulfamoylchloride (1.34 g, 4.75 mmol), dried potassium fluoride (1.38 g, 23.7 mmol) and 18-crown-6 (0.126 g, 0.475 mmol) were suspended in acetonitrile (40 mL). After 30 min the reaction mixture changed color to orange and it was stirred for 3 d at room temperature. The green suspension was filtered and all volatiles were removed from the filtrate in vacuo. The green residue was dissolved in diethyl ether (30 mL). Hydrogen chloride was passed through the solution

for five minutes resulting in a color change to red. Precipitated potassium chloride was separated by filtration and diethyl ether was removed from the filtrate in vacuo. The residue was sublimed (65°C , 1.8×10^{-2} mbar) to yield HN(Pf)(Sf) (0.901 g, 72%) as a colorless crystalline solid. M.p. 35°C ; ^1H NMR (300 MHz, C_6D_6 , 25°C , TMS): $\delta = 4.92$ ppm (s, 1 H, NH); ^{13}C NMR (126 MHz, C_6D_6 , 25°C , TMS): $\delta = 144.7$ (d, $^1\text{J}(\text{C},\text{F}) = 254.2$ Hz, CF_{Ar}), 141.8 (d, $^1\text{J}(\text{C},\text{F}) = 256.8$ Hz, CF_{Ar}), 137.8 (d, $^1\text{J}(\text{C},\text{F}) = 252.1$ Hz, CF_{Ar}), 109.2 ppm (d, $^2\text{J}(\text{C},\text{F}) = 14.9$ Hz, $ipso\text{-C}$); ^{19}F NMR (471 MHz, C_6D_6 , 25°C , FCCl_3): $\delta = 54.2$ (m, 1 F, $-\text{SO}_2\text{F}$), -145.0 (m, 2 F, $o\text{-F}$), -150.7 (t, $^3\text{J}(\text{F},\text{F}) = 22.9$ Hz, 1 F, $p\text{-F}$), -160.9 ppm (t, $^3\text{J}(\text{F},\text{F}) = 21.4$ Hz, 2 F, $m\text{-F}$); IR: $\tilde{\nu} = 411$ (m), 456 (m), 495 (m), 533 (m), 562 (s), 584 (w), 621 (m), 768 (s), 804 (s), 929 (m), 986 (s), 1037 (m), 1074 (m), 1164 (w), 1214 (s), 1319 (m), 1355 (w), 1462 (s), 1514 (s), 1652 (w), 3305 cm^{-1} (m, NH); (–)ESI-MS (MeCN): m/z (%): 264 (100) [$M-\text{H}^+$], 249 (25) [$M-\text{H}^+-\text{O}$]; HRMS ((–)ESI (MeCN)): m/z calcd for $\text{C}_6\text{F}_6\text{NO}_2\text{S}^-$ 263.9559 [$M-\text{H}^+$]; found: 263.9559; elemental analysis calcd. (%) for $\text{C}_6\text{HF}_6\text{NO}_2\text{S}$: C 27.18, H 0.38, N 5.28, S 12.09; found: C 27.25, H 0.40, N 5.47, S 12.49.

X-ray structure analysis

IPDS I and IPDS II (Stoe) diffractometers were used for data collection by the x-ray department at the Philipps-Universität Marburg (Dr. K. Harms, G. Geiseler, M. Marsch, and R. Riedel). Data collection, reduction, and cell refinement were performed with Stoe IPDS Software. Structures were solved with SIR92,^[48] SIR97^[49] or SIR2004^[50] and refined with SHEXL-97^[51]. Absorption correction was performed with semi-empirical methods within WinGX (multiscan^[52] or Gaussian).^[53]

Carbon-bound hydrogen atoms were calculated in their idealized positions and refined with fixed isotropic thermal parameters. Hydrogen atoms connected to heteroatoms were located on the Fourier map and refined isotropically. In case of HN(Pf)(Nf), HN(Pf)(Sf), and HN(Pf)($\text{SO}_2\text{N}(\text{Pf})(\text{Sf})$) NH distances were restrained at 87 pm using the DFIX command. All molecular structures were illustrated with Diamond 3^[54] using thermal ellipsoids at the 30% probability level for all non-hydrogen atoms and fixed radii for heteroatom-bonded hydrogen atoms. Carbon-bonded hydrogen atoms are omitted for clarity.

Crystal data and experimental conditions are listed in S-Table 0 (see the Supporting Information). Selected bonding and nonbonding distances and angles with standard deviations in parentheses are collected in Table 1. The corresponding CIF files providing full information concerning the molecular structures and experimental conditions are deposited at the Cambridge Crystallographic Data Center.

5. Computational Details

The program TURBOMOLE^[55] was used for DFT and MP2 calculations. By default, vibrational, rotational, and translational, as well as entropic corrections to thermochemistry were calculated with BP86^[56]/def-TZVP^[57] using the FREEH tool (unscaled).^[58] For this, the vibrational frequencies were determined analytically with the AO-FORCE^[59] module. We ensured that all structures are true minima and show no imaginary frequencies. For obtaining absolute energies, we applied the optimized structures gained from the B3LYP^[56a,60] hybrid functional in combination with augmented correlation-consistent triple-zeta basis sets of Dunning et al.^[61] (aug-cc-pVTZ). We then calculated a MP2(FC)^[62]/aug-cc-pVTZ single point on the B3LYP/aug-cc-pVTZ geometry and called the method "M1". When available, we used the RI approximation for DFT^[63] and

MP2.^[64] As an alternative^[65] we applied the RIJK^[66] approach for B3LYP/aug-cc-pVTZ. For our extensive model validation (see the Supporting Information) we applied various combinations of density functionals and MP2(FC) with different basis sets, in addition to the methods mentioned above including the hybrid-functional PBE0^[67] and the basis sets def2-TZVPP,^[68] def2-QZVPP^[68] and aug-cc-pVQZ.^[61]

We also used the Gaussian packages^[69] to calculate the compound approaches G3^[70] and G3MP2.^[71] Our recently introduced modified G3 (G3_{mod})^[29] served as reference method for model validation (besides the experimental values) by means of the GA values of the investigated acids and for the isodesmic calculations. Thus, we improved G3MP2 analogously to G3_{mod} by using thermochemical corrections at the BP86/def-TZVP level. The definition of the G3MP2_{mod} Gibbs energies at standard conditions follows Equation (2):

$$G^\circ(G3MP2_{\text{mod}}) = G3MP2(0K) - ZPE(G3MP2) + \text{Free H energy} \\ + RT - T \cdot \text{Free H entropy} \quad (2)$$

As described in section 2.2, Gibbs solvation energies were calculated with COSMO^[72] as implemented in TURBOMOLE at the BP86/def-TZVP level of theory. We employed default COSMO options as well as default optimized COSMO radii. For control purposes we also applied COSMO at the B3LYP/aug-cc-pVTZ level and PCM^[73] as implemented in Gaussian 03 at the BP86/TZVP level. By default all Gibbs solvation energy calculations were performed in C₁ symmetry and Gaussian 03 reference values were adopted for the dielectric constants. Note: The value yielded from COSMO respectively PCM reflects a transfer from a 1 M ideal gas (24.79 bar at 298.15 K) to a 1 M ideal solution. To obtain the Gibbs standard solvation energy $\Delta_{\text{solv}}G^\circ$ (transfer from an ideal gas at 1 bar to a 1 M ideal solution) we therefore had to add $RT \ln 24.79 = 7.96 \text{ kJ mol}^{-1}$.^[29]

Acknowledgements

This work was supported by the Universities of Marburg and Freiburg, the DFG and the ERC in the Advanced Grant Uni-Chem. The work of I.L., K.K. and J.S. was supported by the Institutional Funding Project IUT20-14 from the Estonian Ministry of Education and Science and the Estonian Centre of Excellence HIGHTECHMAT (SLOKT117T). The financial support of the Fonds der Chemischen Industrie (doctoral scholarship for J.F.K) is gratefully acknowledged. We thank Martin Scott for his synthetic contribution and Lars Hendrik Finger (both University of Marburg) for valuable support with crystal structure refinement. The results and discussion of the synthetic and crystallographic part are, with some modifications, part of the doctoral thesis of Julius F. Kögel, University of Marburg, 2014: Bisphosphazene Proton Sponges and Metal Perfluoroanilides: Ligand Design for Brønsted Superbases and Lewis Superacids. The results and discussion of the computations are, with some modifications, part of the doctoral thesis of Sascha K. Goll, University of Freiburg, 2013: Quantum Chemical Calculations Towards a Unified pH Scale for All Phases.

Keywords: acidity • analytical methods • anions • density functional calculations • sulfonamides

- [1] a) J. Foropoulos, Jr., D. D. DesMarteau, *Inorg. Chem.* **1984**, *23*, 3720–3723; b) D. D. DesMarteau, M. Witz, *J. Fluorine Chem.* **1991**, *52*, 7–12.
- [2] a) I. A. Koppel, R. W. Taft, F. Anvia, S.-Z. Zhu, L.-Q. Hu, K.-S. Sung, D. D. DesMarteau, L. M. Yagupolskii, Y. L. Yagupolskii, N. V. Ignat'ev, N. V. Kondratenko, A. Y. Volkonskii, V. M. Vlasov, R. Notario, P.-C. Maria, *J. Am. Chem. Soc.* **1994**, *116*, 3047–3057; b) P. Burk, I. A. Koppel, I. Koppel, L. M. Yagupolskii, R. W. Taft, *J. Comput. Chem.* **1996**, *17*, 30–41; c) A. Kütt, T. Rodima, J. Saame, E. Raamat, V. Määmet, I. Kaljurand, I. A. Koppel, R. Y. Garlyauskayte, Y. L. Yagupolskii, L. M. Yagupolskii, E. Bernhardt, H. Willner, I. Leito, *J. Org. Chem.* **2011**, *76*, 391–395; d) I. Rey, P. Johansson, J. Lindgren, J. C. Lassègues, J. Grondin, L. Servant, *J. Phys. Chem. A* **1998**, *102*, 3249–3258.
- [3] D. H. Ryu, E. J. Corey, *J. Am. Chem. Soc.* **2003**, *125*, 6388–6390.
- [4] T. C. Wabnitz, J. B. Spencer, *Org. Lett.* **2003**, *5*, 2141–2144.
- [5] L. Zhang, S. A. Kozmin, *J. Am. Chem. Soc.* **2004**, *126*, 10204–10205.
- [6] G. B. Rowland, H. Zhang, E. B. Rowland, S. Chennamadhavuni, Y. Wang, J. C. Antilla, *J. Am. Chem. Soc.* **2005**, *127*, 15696–15697.
- [7] a) A. Noda, M. A. B. H. Susan, K. Kudo, S. Mitsushima, K. Hayamizu, M. Watanabe, *J. Phys. Chem. B* **2003**, *107*, 4024–4033; b) J. G. Huddleston, A. E. Visser, W. M. Reichert, H. D. Willauer, G. A. Broker, R. D. Rogers, *Green Chem.* **2001**, *3*, 156–164.
- [8] a) D. R. MacFarlane, P. Meakin, J. Sun, N. Amini, M. Forsyth, *J. Phys. Chem. B* **1999**, *103*, 4164–4170; b) H. Jin, B. O'Hare, J. Dong, S. Arzhantsev, G. A. Baker, J. F. Wishart, A. J. Benesi, M. Maroncelli, *J. Phys. Chem. B* **2008**, *112*, 81–92.
- [9] N. M. M. Mateus, L. C. Branco, N. M. T. Lourenço, C. A. M. Afonso, *Green Chem.* **2003**, *5*, 347–352.
- [10] R. E. Del Sesto, C. Corley, A. Robertson, J. S. Wilkes, *J. Organomet. Chem.* **2005**, *690*, 2536–2542.
- [11] P. Lozano, J. M. Bernal, R. Piamtongkam, D. Fetzer, M. Vaultier, *ChemSusChem* **2010**, *3*, 1359–1363.
- [12] a) H. Matsumoto, H. Sakaue, K. Tatsumi, M. Kikuta, E. Ishiko, M. Kono, *J. Power Sources* **2006**, *160*, 1308–1313; b) V. Borgel, E. Markevich, D. Aurbach, G. Semrau, M. Schmidt, *J. Power Sources* **2009**, *189*, 331–336; c) P. C. Howlett, D. R. MacFarlane, A. F. Hollenkamp, *Electrochim. Solid-State Lett.* **2004**, *7*, A97–A101; d) T. Frömling, M. Kunze, M. Schönhoff, J. Sundermeyer, B. Roling, *J. Phys. Chem. B* **2008**, *112*, 12985–12990.
- [13] S. Antoniotti, V. Dalla, E. Duñach, *Angew. Chem. Int. Ed.* **2010**, *49*, 7860–7888; *Angew. Chem.* **2010**, *122*, 8032–8060.
- [14] M. Stricker, T. Linder, B. Oelkers, J. Sundermeyer, *Green Chem.* **2010**, *12*, 1589–1598.
- [15] a) A. V. Mudring, *ACS Symp. Ser.* **2007**, *975*, 172–185; b) A.-V. Mudring, A. Babai, S. Arenz, R. Giernoth, K. Binnemanns, K. Driesen, P. Nockemann, *J. Alloys Compd.* **2006**, *418*, 204–208; c) S. Arenz, A. Babai, K. Binnemanns, K. Driesen, R. Giernoth, A.-V. Mudring, P. Nockemann, *Chem. Phys. Lett.* **2005**, *402*, 75–79; d) S. Tang, A. Babai, A. V. Mudring, *Angew. Chem. Int. Ed.* **2008**, *47*, 7631–7634; *Angew. Chem.* **2008**, *120*, 7743–7746.
- [16] a) A. Vij, R. L. Kirchmeier, J. M. Shreeve, R. D. Verma, *Coord. Chem. Rev.* **1997**, *158*, 413–432; b) B. Krumm, A. Vij, R. L. Kirchmeier, J. M. Shreeve, *Inorg. Chem.* **1998**, *37*, 6295–6303; c) A. Guerfi, S. Duchesne, Y. Kobayashi, A. Vijh, K. Zaghib, *J. Power Sources* **2008**, *175*, 866–873.
- [17] a) G. M. Brooke, J. Burdon, M. Stacey, J. C. Tatlow, *J. Chem. Soc.* **1960**, 1768–1771; b) R. Koppang, *Acta Chem. Scand.* **1971**, *25*, 3067–3071.
- [18] a) G. R. Giesbrecht, J. C. Gordon, D. L. Clark, C. A. Hijar, B. L. Scott, J. G. Watkin, *Polyhedron* **2003**, *22*, 153–163; b) P. L. Shutov, S. S. Karlov, K. Harms, M. V. Zabalov, J. Sundermeyer, J. Lorberth, G. S. Zaitseva, *Eur. J. Inorg. Chem.* **2007**, 5684–5692; c) P. L. Shutov, S. S. Karlov, K. Harms, J. Sundermeyer, J. Lorberth, G. S. Zaitseva, *J. Fluorine Chem.* **2009**, *130*, 1017–1021.
- [19] D. R. Click, B. L. Scott, J. G. Watkin, *Chem. Commun.* **1999**, 633–634.
- [20] a) A. Khvorost, P. L. Shutov, K. Harms, J. Lorberth, J. Sundermeyer, S. S. Karlov, G. S. Zaitseva, *Z. Anorg. Allg. Chem.* **2004**, *630*, 885–889; b) P. L. Shutov, S. S. Karlov, K. Harms, D. A. Tyurin, J. Sundermeyer, J. Lorberth, G. S. Zaitseva, *Eur. J. Inorg. Chem.* **2004**, 2498–2503.
- [21] T. Linder, J. Sundermeyer, *Chem. Commun.* **2009**, 2914–2916.
- [22] a) J. R. Sundermeyer, B. Linder, T. Froemling, T. Huber, Vol. EP 2314572 A1 20110427, 2011; b) J. R. Sundermeyer, B. Linder, T. Huber, B. Froemling, T. Huber, Vol. PCT Int. Appl. WO 2011048152 A1 20110428, 2011.
- [23] U. Jäger, W. Sundermeyer, H. Pritzkow, *Chem. Ber.* **1987**, *120*, 1191–1195.

- [24] B. Huber, T. Linder, K. Hormann, T. Frömling, J. Sundermeyer, B. Roling, *Z. Phys. Chem.* **2012**, *226*, 377–390.
- [25] M. Grzegorczyk, M. Gdaniec, *Acta Crystallogr. Sect. C* **2006**, *62*, o419–o422.
- [26] A. Haas, C. Klare, P. Betz, J. Bruckmann, C. Krüger, Y.-H. Tsay, F. Aubke, *Inorg. Chem.* **1996**, *35*, 1918–1925.
- [27] M. Ochiai, T. Okada, N. Tada, A. Yoshimura, K. Miyamoto, M. Shiro, *J. Am. Chem. Soc.* **2009**, *131*, 8392–8393.
- [28] a) I. A. Koppel, F. Anvia, R. W. Taft, *J. Phys. Org. Chem.* **1994**, *7*, 717–724; b) G. Bouchoux, J.-F. Gal, P. C. Maria, J. E. Szulejko, T. B. McMahon, J. Tortajada, A. Luna, M. Yáñez, O. Mó, *J. Phys. Chem. A* **1998**, *102*, 9183–9192; c) P. Burk, I. A. Koppel, A. Rummel, A. Trummal, *J. Phys. Chem. A* **2000**, *104*, 1602–1607; d) I. A. Koppel, P. Burk, I. Koppel, I. Leito, T. Sonoda, M. Mishima, *J. Am. Chem. Soc.* **2000**, *122*, 5114–5124; e) I. A. Koppel, J. Koppel, I. Leito, I. Koppel, M. Mishima, L. M. Yagupolskii, *J. Chem. Soc. Perkin Trans. 2* **2001**, 229–232; f) I. A. Koppel, R. Schwesinger, T. Breuer, P. Burk, K. Herodes, I. Koppel, I. Leito, M. Mishima, *J. Phys. Chem. A* **2001**, *105*, 9575–9586; g) A. A. Kolomeitsev, I. A. Koppel, T. Rodima, J. Barten, E. Lork, G.-V. Röschenthaler, I. Kaljurand, A. Kütt, I. Koppel, V. Mäemets, I. Leito, *J. Am. Chem. Soc.* **2005**, *127*, 17656–17666; h) C. M. Jones, M. Bernier, E. Carson, K. E. Colyer, R. Metz, A. Pawlow, E. D. Wischow, I. Webb, E. J. Andriole, J. C. Poutsma, *Int. J. Mass Spectrom.* **2007**, *267*, 54–62; i) I. Kaljurand, I. A. Koppel, A. Kütt, E.-I. Rööm, T. Rodima, I. Koppel, M. Mishima, I. Leito, *J. Phys. Chem. A* **2007**, *111*, 1245–1250; j) M. Hurtado, M. Yáñez, R. Herrero, A. Guerrero, J. Z. Dávalos, J.-L. M. Abboud, B. Khater, J.-C. Guillemin, *Chem. Eur. J.* **2009**, *15*, 4622–4629; k) A. Kütt, I. Koppel, I. A. Koppel, I. Leito, *ChemPhys-Chem* **2009**, *10*, 499–502; l) I. Leito, E. Raamat, A. Kütt, J. Saame, K. Kipper, I. A. Koppel, I. Koppel, M. Zhang, M. Mishima, L. M. Yagupolskii, R. Y. Garlyauskayte, A. A. Filatov, *J. Phys. Chem. A* **2009**, *113*, 8421–8424; m) M. M. Meyer, X.-B. Wang, C. A. Reed, L.-S. Wang, S. R. Kass, *J. Am. Chem. Soc.* **2009**, *131*, 18050–18051; n) M. Namazian, M. L. Coote, *J. Fluorine Chem.* **2009**, *130*, 621–628; o) I. Leito, I. A. Koppel, P. Burk, S. Tamp, M. Kutsar, M. Mishima, J.-L. M. Abboud, J. Z. Dávalos, R. Herrero, R. Notario, *J. Phys. Chem. A* **2010**, *114*, 10694–10699; p) M. M. Meyer, S. R. Kass, *J. Phys. Chem. A* **2010**, *114*, 4086–4092; q) S. Rayne, K. Forest, *Theor. Chem. Acc.* **2010**, *127*, 697–709; r) S. Rayne, K. Forest, *J. Mol. Struct. THEOCHEM* **2010**, *956*, 83–96; s) L. Lipping, A. Kütt, K. Kaupmees, I. Koppel, P. Burk, I. Leito, I. A. Koppel, *J. Phys. Chem. A* **2011**, *115*, 10335–10344; t) R. A. Kunetskiy, S. M. Polyakova, J. Vavřík, I. Čísařová, J. Saame, E. R. Nerut, I. Koppel, I. A. Koppel, A. Kütt, I. Leito, I. M. Lyapkalo, *Chem. Eur. J.* **2012**, *18*, 3621–3630.
- [29] D. Himmel, S. K. Goll, I. Leito, I. Krossing, *Chem. Eur. J.* **2011**, *17*, 5808–5826.
- [30] a) A. C. Lee, G. M. Crippen, *J. Chem. Inf. Model.* **2009**, *49*, 2013–2033; b) J. Ho, M. L. Coote, *Theor. Chem. Acc.* **2010**, *125*, 3–21; c) J. Ho, M. L. Coote, *WIREs Comput. Mol. Sci.* **2011**, *1*, 649–660; d) Y. E. Zevatskii, D. V. Samoilov, *Russ. J. Org. Chem.* **2011**, *47*, 1445–1467.
- [31] a) M. D. Liptak, G. C. Shields, *J. Am. Chem. Soc.* **2001**, *123*, 7314–7319; b) J. R. Pliego, Jr., J. M. Riveros, *J. Phys. Chem. A* **2002**, *106*, 7434–7439; c) C. P. Kelly, C. J. Cramer, D. G. Truhlar, *J. Phys. Chem. A* **2006**, *110*, 2493–2499; d) V. S. Bryantsev, M. S. Diallo, W. A. Goddard III, *J. Phys. Chem. A* **2007**, *111*, 4422–4430.
- [32] a) B. Kovačević, Z. B. Maksić, *Org. Lett.* **2001**, *3*, 1523–1526; b) D. M. Chipman, *J. Phys. Chem. A* **2002**, *106*, 7413–7422; c) G. I. Almerindo, D. W. Tondo, J. R. Pliego, Jr., *J. Phys. Chem. A* **2004**, *108*, 166–171; d) Y. Fu, L. Liu, R.-Q. Li, R. Liu, Q.-X. Guo, *J. Am. Chem. Soc.* **2004**, *126*, 814–822; e) A. M. Magill, K. J. Cavell, B. F. Yates, *J. Am. Chem. Soc.* **2004**, *126*, 8717–8724; f) Y. Fu, L. Liu, H.-Z. Yu, Y.-M. Wang, Q.-X. Guo, *J. Am. Chem. Soc.* **2005**, *127*, 7227–7234; g) R. Vianello, Z. B. Maksić, *Tetrahedron Lett.* **2005**, *46*, 3711–3713; h) R. Vianello, Z. B. Maksić, *Mol. Phys.* **2005**, *103*, 209–219; i) F. A. Villamena, J. K. Merle, C. M. Hadad, J. L. Zweier, *J. Phys. Chem. A* **2005**, *109*, 6083–6088; j) Y. Fu, L. Liu, Y.-M. Wang, J.-N. Li, T.-Q. Yu, Q.-X. Guo, *J. Phys. Chem. A* **2006**, *110*, 5874–5886; k) J. P. Holland, J. C. Green, J. R. Dilworth, *Dalton Trans.* **2006**, 783–794; l) J.-N. Li, L. Liu, Y. Fu, Q.-X. Guo, *Tetrahedron* **2006**, *62*, 4453–4462; m) X.-J. Qi, L. Liu, Y. Fu, Q.-X. Guo, *Organometallics* **2006**, *25*, 5879–5886; n) X.-J. Qi, Y. Fu, L. Liu, Q.-X. Guo, *Organometallics* **2007**, *26*, 4197–4203; o) K. Shen, Y. Fu, J.-N. Li, L. Liu, Q.-X. Guo, *Tetrahedron* **2007**, *63*, 1568–1576; p) A. Yu, Y. Liu, Z. Li, J.-P. Cheng, *J. Phys. Chem. A* **2007**, *111*, 9978–9987; q) F. Ding, J. M. Smith, H. Wang, *J. Org. Chem.* **2009**, *74*, 2679–2691; r) F. Eckert, I. Leito, I. Kaljurand, A. Kütt, A. Klamt, M. Diedenhofen, *J. Comput. Chem.* **2009**, *30*, 799–810; s) Y. Fu, H.-J. Wang, S.-S. Chong, Q.-X. Guo, L. Liu, *J. Org. Chem.* **2009**, *74*, 810–819; t) Z. Glasovac, M. Eckert-Maksić, Z. B. Maksić, *New J. Chem.* **2009**, *33*, 588–597; u) A. Trummal, A. Rummel, E. Lippmaa, P. Burk, I. A. Koppel, *J. Phys. Chem. A* **2009**, *113*, 6206–6212; v) X.-Y. Huang, H.-J. Wang, J. Shi, *J. Phys. Chem. A* **2010**, *114*, 1068–1081; w) M. Uudsemaa, T. Kanger, M. Lopp, T. Tamm, *Chem. Phys. Lett.* **2010**, *485*, 83–86; x) R. Vianello, Z. B. Maksić, *J. Org. Chem.* **2010**, *75*, 7670–7681; y) X.-Q. Zhu, C.-H. Wang, H. Liang, *J. Org. Chem.* **2010**, *75*, 7240–7257; z) B. H. Solis, S. Hammes-Schiffer, *Inorg. Chem.* **2011**, *50*, 11252–11262.
- [33] a) J. Tomasi, *Theor. Chem. Acc.* **2004**, *112*, 184–203; b) J. Tomasi, B. Mennucci, R. Cammi, *Chem. Rev.* **2005**, *105*, 2999–3093; c) J. Ho, A. Klamt, M. L. Coote, *J. Phys. Chem. A* **2010**, *114*, 13442–13444.
- [34] J. R. Pliego, Jr., J. M. Riveros, *J. Phys. Chem. A* **2001**, *105*, 7241–7247.
- [35] D. Himmel, S. K. Goll, I. Leito, I. Krossing, *Angew. Chem. Int. Ed.* **2010**, *49*, 6885–6888; *Angew. Chem.* **2010**, *122*, 7037–7040.
- [36] A. Kütt, I. Leito, I. Kaljurand, L. Sooväli, V. M. Vlasov, L. M. Yagupolskii, I. A. Koppel, *J. Org. Chem.* **2006**, *71*, 2829–2838.
- [37] J. F. Kögel, L. H. Finger, N. Frank, J. Sundermeyer, *Inorg. Chem.* **2014**, *53*, 3839–3846.
- [38] A. Kütt, V. Movchun, T. Rodima, T. Dansauer, E. B. Rusanov, I. Leito, I. Kaljurand, J. Koppel, V. Pihl, I. Koppel, G. Ovsjannikov, L. Toom, M. Mishima, M. Medebielie, E. Lork, G.-V. Röschenthaler, I. A. Koppel, A. A. Kolomeitsev, *J. Org. Chem.* **2008**, *73*, 2607–2620.
- [39] Original data taken from T. B. Douglas, *J. Am. Chem. Soc.* **1948**, *70*, 2001; reworked by NIST Chemistry WebBook, NIST Standard Reference Database Number 69, <http://webbook.nist.gov>.
- [40] Original data taken from W. E. Putnam, D. M. McEachern, Jr., J. E. Kilpatrick, *J. Chem. Phys.* **1965**, *42*, 749; reworked by NIST Chemistry WebBook, NIST Standard Reference Database Number 69, <http://webbook.nist.gov>.
- [41] Gaussian 03 reference values were adopted for the dielectric constants.
- [42] a) I. Koppel, J. Koppel, I. Leito, V. Pihl, L. Grehn, U. Ragnarsson, *J. Chem. Res. Synop.* **1994**, 212–213; b) I. Koppel, J. Koppel, P.-C. Maria, J.-F. Gal, R. Notario, V. M. Vlasov, R. W. Taft, *Int. J. Mass Spectrom. Ion Processes* **1998**, *175*, 61–69.
- [43] V. M. Vlasov, M. I. Terekhova, E. S. Petrov, A. I. Shatenshtein, G. G. Yakobson, *Zh. Org. Khim.* **1981**, *17*, 2025–2031.
- [44] Note: As mentioned above, the contact ion pair formation of H–BTFSI-DMSO in DMSO during optimization yields an increase of 9.5 pK_a units, but there are energy differences between the vCCC and the rCCC model at other parts of the BFHCs.
- [45] K. Kaupmees, N. Tolstoluzhsky, S. Raja, M. Rueping, I. Leito, *Angew. Chem. Int. Ed.* **2013**, *52*, 11569–11572; *Angew. Chem.* **2013**, *125*, 11783–11786.
- [46] In this case, a “HNTf₂ molecule in DMSO” means a Lewisacid-base adduct Me2→HNTf₂ and not an isolated HNTf₂ molecule.
- [47] G. Brauer, *Handbuch der Präparativen Anorganischen Chemie*, Ferdinand Enke Verlag, Stuttgart, **1975**, pp. 712–723.
- [48] A. Altomare, G. Casciaro, C. Giacovazzo, A. Guagliardi, *J. Appl. Crystallogr.* **1993**, *26*, 343–350.
- [49] A. Altomare, M. C. Burla, M. Camalli, G. L. Casciaro, C. Giacovazzo, A. Guagliardi, A. G. G. Moliterni, G. Polidori, R. Spagna, *J. Appl. Crystallogr.* **1999**, *32*, 115–119.
- [50] M. C. Burla, R. Caliandro, M. Camalli, B. Carrozzini, G. L. Casciaro, L. De Caro, C. Giacovazzo, G. Polidori, R. Spagna, *J. Appl. Crystallogr.* **2005**, *38*, 381–388.
- [51] G. Sheldrick, *Acta Crystallogr. Sect. A* **2008**, *64*, 112–122.
- [52] R. H. Blessing, *Acta Crystallogr. Sect. A* **1995**, *51*, 33–38.
- [53] P. Coppens in *Crystallographic Computing* (Eds.: F. R. Ahmed, S. R. Hall, P. C. Huber), Munksgaard, Copenhagen, **1970**, pp. 225–270.
- [54] Diamond 3; K. Brandenburg, H. Putz, v3.2i ed., Crystal Impact GbR, Bonn, Germany, **2012**.
- [55] a) R. Ahlrichs, M. Bär, M. Häser, H. Horn, C. Kölmel, *Chem. Phys. Lett.* **1989**, *162*, 165–169; b) O. Treutler, R. Ahlrichs, *J. Chem. Phys.* **1995**, *102*, 346–354.
- [56] a) A. D. Becke, *Phys. Rev. A* **1988**, *38*, 3098–3100; b) J. P. Perdew, *Phys. Rev. B* **1986**, *33*, 8822–8824; c) J. P. Perdew, *Phys. Rev. B* **1986**, *34*, 7406–7406.
- [57] A. Schäfer, H. Horn, R. Ahlrichs, *J. Chem. Phys.* **1992**, *97*, 2571–2577.

- [58] Coincidentally for BP86/def-TZVP frequencies the scaling factor is very close to unity.
- [59] a) P. Deglmann, F. Furche, *J. Chem. Phys.* **2002**, *117*, 9535–9538; b) P. Deglmann, F. Furche, R. Ahlrichs, *Chem. Phys. Lett.* **2002**, *362*, 511–518.
- [60] a) A. D. Becke, *J. Chem. Phys.* **1993**, *98*, 5648–5652; b) C. Lee, W. Yang, R. G. Parr, *Phys. Rev. B* **1988**, *37*, 785–789.
- [61] a) T. H. Dunning, Jr., *J. Chem. Phys.* **1989**, *90*, 1007–1023; b) R. A. Kendall, T. H. Dunning, Jr., R. J. Harrison, *J. Chem. Phys.* **1992**, *96*, 6796–6806.
- [62] The core orbitals were retained frozen, only the valence shell orbitals were considered.
- [63] a) K. Eichkorn, O. Treutler, H. Öhm, M. Häser, R. Ahlrichs, *Chem. Phys. Lett.* **1995**, *240*, 283–290; b) K. Eichkorn, O. Treutler, H. Öhm, M. Häser, R. Ahlrichs, *Chem. Phys. Lett.* **1995**, *242*, 652–660; c) K. Eichkorn, F. Weigend, O. Treutler, R. Ahlrichs, *Theor. Chem. Acc.* **1997**, *97*, 119–124.
- [64] a) F. Weigend, M. Häser, *Theor. Chem. Acc.* **1997**, *97*, 331–340; b) F. Weigend, M. Häser, H. Patzelt, R. Ahlrichs, *Chem. Phys. Lett.* **1998**, *294*, 143–152.
- [65] For B3LYP/aug-cc-pVTZ currently no RI approximation for sulfur is available. So we first performed the calculations without any auxiliary basis sets for the respective geometry optimizations. Later we switched to the computationally less “expensive” RIJK approximation, which is available for sulfur too, to calculate the anion-solvent adducts as well as the isodesmic model systems of the anions and their solvent adducts. The RIJK approximation was also used for all B3LYP/aug-cc-pVTZ calculations regarding the acidity of HN(Pf)(Sf). We performed control accounts with RIJK versus without RIJK for the anions of the weakest and the strongest acid (NPf_2^- respectively NTf_2^-) as well as for MeCN and DMSO. We found deviations (see Supporting Information) up to 0.2 kJ mol^{-1} for the energies of the optimized B3LYP/aug-cc-pVTZ structures and up to 0.1 kJ mol^{-1} for the (RI-)MP2(FC)/aug-cc-pVTZ single points based on this geometries as employed in our M1 method. We decided to neglect the latter.
- [66] F. Weigend, *Phys. Chem. Chem. Phys.* **2002**, *4*, 4285–4291.
- [67] a) J. P. Perdew, K. Burke, M. Ernzerhof, *Phys. Rev. Lett.* **1996**, *77*, 3865–3868; b) J. P. Perdew, K. Burke, M. Ernzerhof, *Phys. Rev. Lett.* **1997**, *78*, 1396; c) C. Adamo, V. Barone, *J. Chem. Phys.* **1999**, *110*, 6158–6170.
- [68] F. Weigend, R. Ahlrichs, *Phys. Chem. Chem. Phys.* **2005**, *7*, 3297–3305.
- [69] a) M. J. Frisch, G. W. Trucks, H. B. Schlegel, G. E. Scuseria, M. A. Robb, J. R. Cheeseman, J. J. A. Montgomery, T. Vreven, K. N. Kudin, J. C. Burant, et al., Gaussian 03, Revision D.02, Gaussian, Inc., Wallingford CT, **2004** (for full reference, see the Supporting Information); b) M. J. Frisch, G. W. Trucks, H. B. Schlegel, G. E. Scuseria, M. A. Robb, J. R. Cheeseman, G. Scalmani, V. Barone, B. Mennucci, G. A. Petersson, et al., Gaussian 09, revision B.01; Gaussian, Inc.: Wallingford, CT, **2010** (for full reference see the Supporting Information).
- [70] L. A. Curtiss, K. Raghavachari, P. C. Redfern, V. Rassolov, J. A. Pople, *J. Chem. Phys.* **1998**, *109*, 7764–7776.
- [71] L. A. Curtiss, P. C. Redfern, K. Raghavachari, V. Rassolov, J. A. Pople, *J. Chem. Phys.* **1999**, *110*, 4703–4709.
- [72] a) A. Klamt, G. Schüürmann, *J. Chem. Soc. Perkin Trans. 2* **1993**, 799–805; b) A. Schäfer, A. Klamt, D. Sattel, J. C. W. Lohrenz, F. Eckert, *Phys. Chem. Chem. Phys.* **2000**, *2*, 2187–2193.
- [73] a) S. Miertus, E. Scrocco, J. Tomasi, *Chem. Phys.* **1981**, *55*, 117–129; b) M. Cossi, G. Scalmani, N. Rega, V. Barone, *J. Chem. Phys.* **2002**, *117*, 43–54.

Received: September 24, 2014

Published online on February 26, 2015